PERGAMON

Quaternary Science Reviews 22 (2003) 1737–1756

QSR

Palaeoflood record of the Tagus River (Central Spain) during the Late Pleistocene and Holocene

Gerardo Benito[a,*], Alfonso Sopeña[b], Yolanda Sánchez-Moya[c], María J. Machado[d], Alfredo Pérez-González[d]

[a] *CSIC-Centro de Ciencias Medioambientales, Serrano 115 bis, 28006 Madrid, Spain*
[b] *Instituto de Geología Económica, CSIC-UCM, Facultad de Ciencias Geológicas, Universidad Complutense de Madrid, 28040 Madrid, Spain*
[c] *Departamento de Estratigrafía, Instituto de Geología Económica, CSIC-UCM, Facultad de Ciencias Geológicas, Universidad Complutense de Madrid, 28040 Madrid, Spain*
[d] *Departamento de Geodinámica, Facultad de Ciencias Geológicas, Universidad Complutense de Madrid, 28040 Madrid, Spain*

Received 13 September 2002; accepted 18 April 2003

Abstract

Palaeoflood hydrology of the Tagus River (Central Spain) was reconstructed from slackwater deposits and palaeostage indicators in two canyon reaches located at El Puente del Arzobispo in the central part of the catchment (35,000 km^2 in drainage area) and in Alcántara, at the lower part of the catchment (52,000 km^2 in drainage area) near the Portuguese border. The palaeoflood record, with more than 80 flood events, shows clusters of floods at specific periods from 9440 to 9210 ^{14}C yr BP (8540–8110 BC), 8500 to 8000 ^{14}C yr BP (7500–7000 BC), ~6750 ^{14}C yr BP (~5000 BC), 1200 to 950 ^{14}C yr BP (AD 785–1205), ~410 ^{14}C yr BP (AD 1450–1500), 170 to 80 ^{14}C yr BP (AD 1670–1950). The largest flood(s) occurred during the periods 9440 to 9210 ^{14}C yr BP, ~6750 ^{14}C yr BP and 1200 to 950 ^{14}C yr BP reaching minimum discharge estimates of between 4000 and 4100 m^3 s^{-1} in the El Puente del Arzobispo reach and 13,700–15,000 m^3 s^{-1} in the Alcántara reach. These periods with increased flood magnitude and/or frequency in the Tagus River are strongly related to increased moisture influx and winter precipitation in the Iberian Peninsula, especially in the western zone. Proxy records sensitive to winter precipitation such as lake levels and vegetation changes (indicated by pollen records) are in good agreement with the clusters of floods found in the Tagus River. This flood variability seems to correspond to changes in the prevailing atmospheric circulation pattern affecting the Iberian Peninsula.

1. Introduction

During the 20th Century, most of Europe has experienced a temperature increase of about 0.8°C on average (IPCC, 2001), and even larger over the Iberian Peninsula (Onate and Pou, 1996). Global circulation model (GCM) projections for the future, applied to regions such as Europe, are still too uncertain to draw all but highly tentative conclusions predicting changes on rainfall patterns. There is also an open debate over changes in the frequency of future floods. For a scenario of increased rainfall during periods when soils are saturated (i.e. winter and spring) along with earlier snowmelt, the frequency and severity of floods might be increased, especially in large river basins of Central-Western Europe in winter (IPCC, 1996). Expected increased temperatures in summer could lead to higher local precipitation extremes and associated flood risks in small catchments. Other scenarios can be predicted for different regions such as the Mediterranean, indicating that the flood response to global warming based exclusively on GCMs is still far from well understood.

Some insight into flood–climate relations is provided by past flood data, both from palaeoflood and historical flood records. Historical information provides a catalogue of the largest floods occurring during periods of settlement (Benito et al., 1996, 2003b; Barriendos and Martín-Vide, 1998), while palaeoflood investigations based on geological indicators can document the magnitude of these large floods over a certain period of time (from decades to millennia). Thus, the length of the extreme flood record is not limited to the few dozen

*Corresponding author. Tel.: +34-1-562-5020; fax: +34-1-564-0800.
E-mail address: benito@ccma.csic.es (G. Benito).

0277-3791/03/$ - see front matter © 2003 Elsevier Ltd. All rights reserved.
doi:10.1016/S0277-3791(03)00133-1

years of the conventional (instrumental) record, but may be extended to cover thousands of years.

Stadial and interstadial periods of the Late Pleistocene show some of the most significant rapid climatic change events (such as the Younger Dryas, with a mean summer temperature 8°C cooler than the present), with transitions occurring over very short time spans (on the decade to century time scale; Allen et al., 1996). For the Holocene, multiple scenarios of climate change have been defined and include temperature changes of ± 2°C with respect to present temperatures, and mean precipitation changes of some 20% (Knox, 1993). It is true that there are still many doubts as to how these changes occurred and to their spacio-temporal effects on the magnitude and frequency of floods. However, it is clear that using past climatic scenarios is a viable option in understanding the potential disruptions of the water cycle during future global climatic change.

It has been established that floods are highly sensitive to even modest changes in climate (Knox, 1993, 2000; Ely, 1997). Palaeoflood studies are based on event-related records that represent an immediate response to a climate-related extreme (intense precipitation over extensive zones), which can be quantified in terms of magnitude and frequency. Indeed, traditional methods of analysing Holocene climatic change such as the use of pollen records, may show low sensitivity to short duration climatic change. Even in the case of lake level variability, hydrologic responses and their responsible climatic change may not be contemporary. Palaeoflood records cannot be considered a proxy-record but may be taken as real evidence for the occurrence of an individual hydrological event. In large river catchments such as that of the Tagus River (80,000 km^2), high precipitation for weeks or even months is required to produce a flood event and raise the stage up to 35 m higher than normal, producing peak discharges up to 50 times the mean. Clusters of floods over certain periods of the Late Pleistocene–Holocene are likely to be linked to regional and global climatic variation over the last 15,000 years.

Palaeohydrological analysis permits the identification of periods showing a greater frequency of a particular behaviour, or pattern, of global circulation of the atmosphere and, in some way, allows the estimation of the size of these anomalies over time (Hirschboeck, 1991). Relationships between changes in climate and flood frequency have been established for certain areas including southwestern USA, Australia, China and South Africa (Knox, 1985, 1993, 2000; Baker, 1987; Pickup et al., 1988; Ely et al., 1993; Ely, 1997). As for climate, the hydrologic response to changes in global circulation shows regional variation and may have considerable impact on this scale. Past regional and global spatial and temporal patterns of flooding show how past climatic changes provoked strong in-phase or out-of-phase relations between regions as well as a diachronous response across regions (Knox, 2000). Distribution patterns corresponding to either in-phase or out-of-phase situations similarly suggest that these alterations in atmospheric circulation play a significant role on the global scale. As we continue to understand more about the patterns of climatic change for the different regions in the world, we will improve our understanding of potential responses of extreme events to the different forecasted scenarios of global warming models.

This paper deals with the application and development of new methodologies for the reconstruction of the high-magnitude flood record of the Tagus Basin over the last 15,000 yr. The main objectives are: (1) reconstruction of the catalogue of major flood events using the stratigraphic record of slackwater flood deposits, (2) study of palaeoflood hydraulics associated with these floods with estimation of flood peak discharges, (3) analysis of palaeoclimatic conditions related to the palaeoflood periods derived from palynological data and other proxy-records of the Iberian Peninsula and northern Africa, and (4) evaluation of relations between climatic variability and changes in flood frequency and magnitude. These flood clusters identified for some periods of the Late Pleistocene and Holocene can be linked to climatic and/or environmental changes on the regional and global scale.

2. Study areas

The Tagus River drains the central part of the Spanish Plateau (Meseta), with an E–W elongated basin with headwaters in the Iberian Range and its mouth into the Atlantic Ocean in Lisbon (Fig. 1). It is the longest river of the Iberian Peninsula (1200 km) and the third largest in catchment area (81,947 km^2). The Tagus Basin is limited by the Central Range to the north, the Iberian Range to the east and the Toledo Mountains to the south. In the area limited by these mountain ranges and in the first 300 km of its course, the Tagus crosses a tectonic depression filled by continental Tertiary sandstones, shales, marls, gypsum and limestones. Here, the river has developed a complete sequence of terrace surfaces and a wide floodplain. From Talavera de la Reina to Santarem (entrance of the Lisbon estuary), the Tagus River has incised into the bedrock composed of Palaeozoic rocks (granite, slate, schist, quartzite), forming a series of deep gorges.

Present-day mean discharge close to the river mouth in Lisbon is 500 m^3 s^{-1}, where the major contribution is made by the tributaries draining the Central Range. These open into the middle-low reaches of the Tagus. Hydrologically, the Tagus River is characterised by

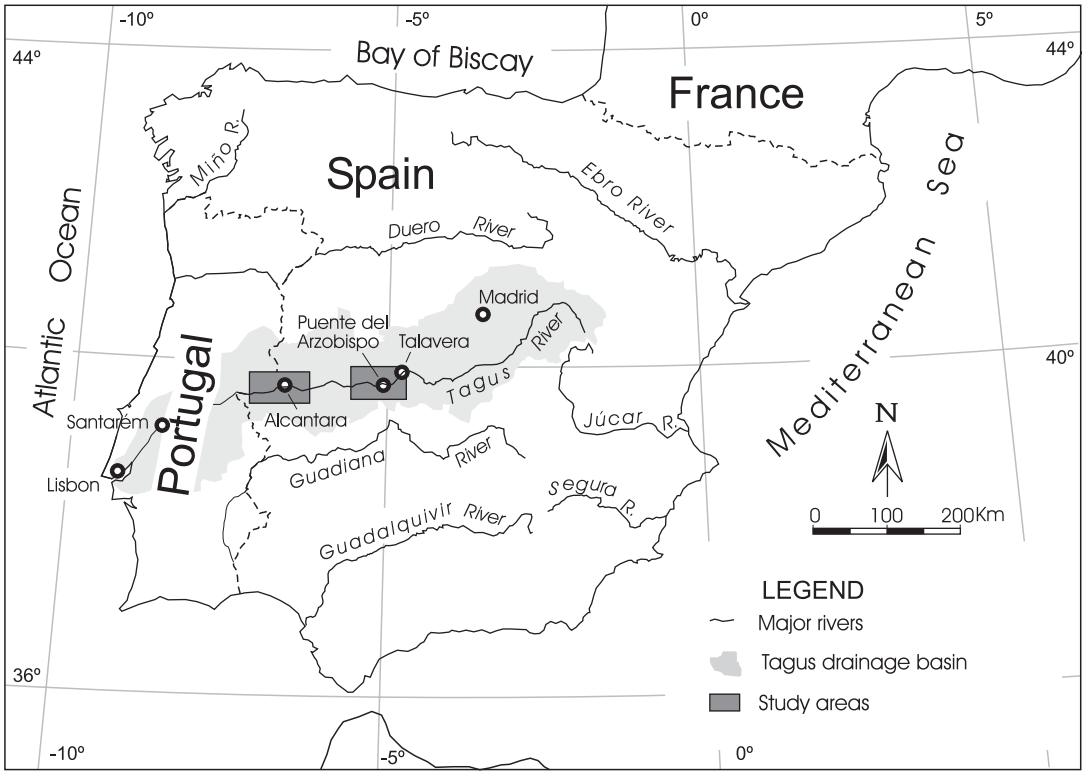

Fig. 1. Main rivers in Spain, and location of the study areas within the Tagus Basin.

extreme seasonal and annual variability including severe floods with peak discharges more than 30 times the mean. The Tagus River regime is influenced by Atlantic fronts which cross the Iberian Peninsula mostly during winter. The eastern and northeastern tributaries have a mixed hydrological regime from snowmelt and rainwaters from the Iberian and eastern Central Range areas, whereas the southern and northwestern tributaries are dominated by rainwaters. General discharge characteristics are: (1) maximum discharge from February to March; (2) minimum discharge in August; (3) a peak in December; and (4) a discharge reduction in January.

The general climate characteristics of the Iberian Peninsula, which also applies for the Tagus River Basin, is characterised by clear seasonal and monthly variability (Capel, 1981). Summers are hot and dry and winters are generally mild and relatively wet. This regime is controlled by two main systems: the subtropical anticyclone of the Azores during summer, and the westerlies, associated with cold fronts, in winter. Some major seasonal trends associated with the frequency of a given circulation pattern may be identified. In the Tagus River, flood producing events are related to a low-pressure cell located southwest of Ireland (Gran Sol) advecting cold fronts into the western part of the Iberian Peninsula with W–E and SW–NE directions. A blocked situation of this low-pressure cell may give rise to persistent precipitation and severe floods in the Tagus Basin (Capel, 1981). Climatic variability through time has given rise to changes in the frequency and severity of circulation patterns producing floods (Benito et al., 1996, 2003b; Barriendos and Martín-Vide, 1998). Therefore, the understanding of the climatic trends and their positive or negative flood signals related to magnitude and frequency through time can be applied to the expected flood response to future climatic changes.

The selected areas are located in a 350 km reach along the central and lower parts of the catchment where the Tagus River cuts through deep gorges. Currently, the Tagus River is fully regulated by dams that have inundated most of these gorges. The longest one is the Alcántara reservoir, ca 130 km in length with a maximum volume of 3162 millions of m^3. This reservoir sequence along the Tagus gorge restricts the analysis of slackwater flood deposit sites. This palaeoflood study has been focused in two areas with different hydrological and geomorphological characteristics. The Puente del Arzobispo reach, on granitic bedrock, is ca 60 km downstream of Talavera de la Reina, covering an upstream drainage basin of ca 35,000 km^2 (Fig. 1). The Alcántara reach, on schist and slate rocks, is located near the Portuguese border, ca 200 km downstream from Talavera, and covers a catchment area of 51,958 km^2 (Fig. 1).

3. El Puente del Arzobispo

The Tagus River downstream of El Puente del Arzobispo cuts through granitic rocks and develops into a 125 m deep gorge. The remnants of eroded Pleistocene soils, only 6 m above the present thalweg, indicate that incision of the gorge during the Holocene has been minor. Late Pleistocene and Holocene deposits along the gorge are related to the flood dynamics and to local slope processes. Sudden changes in water stage due to flooding are frequent during winter covering the centennial water mills located along the river. Flooding has left a set of erosional and depositional features, which allow reconstruction of the flood dynamics.

3.1. Flood geomorphology and stratigraphy

In the El Puente del Arzobispo gorge (Fig. 2), depositional environments include areas of (1) channel widening, (2) canyon expansion, (3) bedrock obstacles and (4) lower reaches of tributaries that are subject to back flooding (Benito et al., 2003a). Reduction of velocity is drastic in these areas of ineffective flow (from 1.4–4 m s^{-1} in the main channel to 0.1–0.6 m s^{-1} in protected zones), resulting in rapid deposition of suspended load. These types of sediments known as slackwater deposits have been described by several researchers (e.g. Bretz, 1929; Baker, 1973; Kochel et al., 1982; Baker et al., 1983; O'Connor et al., 1994; Benito et al., 1998, 2003a) as the most useful for the estimation of palaeoflood peak discharge.

Slackwater deposits in the El Puente del Arzobispo gorge are preserved in thick, high-standing terraces or "benches" along channel margins in canyon expansion reaches (Fig. 3), and at tributary mouths. In marginal zones with development during flood stages of more energetic eddies, flood deposits are reworked preserving a "ridge" morphology more typical of eddy bars. Slackwater terraces or "benches" are documented in other palaeoflood studies (Patton et al., 1979; Kochel et al., 1982; Ely and Baker, 1985) and they are developed by standing or slow-moving water which allow a better preservation of flood deposits through time.

Three terraces, each with multiple flood units, were recognised in the study area (Fig. 2). There are two basic assumptions explaining the formation and development of these slackwater terraces (Baker, 1989; House et al., 2002): (1) they are formed by vertical accretion of slackwater sediments deposited by successive floods, that constitute a rising threshold or local censoring level over time, and (2) inset benches are formed when smaller floods are unable to overtop the upper terrace surface. Nevertheless, to understand the complete palaeoflood record preserved along the reach, some considerations regarding the formation and geometry of the flood unit sets within these terraces should be pointed out. Firstly, each terrace containing slackwater flood deposits can be formed by multiple overlapped fill insets, and therefore the bench may contain a complex three-dimensional architecture. In this case, the reconstruction of the complete palaeoflood record requires multiple cuts showing both lateral and vertical relationships of the flood units and of the multiple inserted sedimentary bodies. This complex geometry is frequent in the older flood bench studied in the El Puente del Arzobispo, where excavated trenches located 15 m apart contain very different flood stratigraphy and facies. We assume that the absence of flood deposits representing certain time spans may be related to a large stratigraphical hiatus due to erosion of the benches near the main channel. However, for uneroded sites with a complete stratigraphic record, the absence of sediment deposited during specific parts of the record results from there being a lack of major floods.

3.2. Upper bench

The upper bench is located 17 m above the present channel bottom (Fig. 3). A total of five trenches were cut in this bench along the study reach (profiles 1.1–1.5; Figs. 2 and 4). Profiles 1.3 and 1.5 (Figs. 2 and 4) are 4 m in thickness and they are composed of silt and fine-medium sand units, with very diffuse contacts, brown to yellow in colour, massive structure, extremely consolidated. These profiles 1.3 and 1.5 are overlying granite bedrock and the number of flood units is at least 13. The deposition period for these flood units is well constrained in profile 1.5 (see Table 1) where a mollusc shell was dated at the base of the profile to 9440 ± 50 ^{14}C yr BP (BC 8540–8420) and a second one in the uppermost flood unit to 9210 ± 50 ^{14}C yr BP (BC 8250–8110), showing that this flood bench was built up in a relatively short time.

In a zone of channel expansion located in the uppermost part of the study reach, bench 1 is well developed and it extends for ca 200 m in length (Figs. 2 and 3). This slackwater flood deposit bench (Figs. 2 and 3) exhibits the most complex morpho-sedimentary relations with several fill insets that complicate the reconstruction of the palaeoflood record. Here, profiles 1.1 and 1.2 are about 20 m apart and they show a stratigraphical record of the largest floods, which can be extended back to the Late Pleistocene (Fig. 4). Profile 1.1 is about 8 m in thickness and contains at least 30 stacked flood units with some intercalated slope wash deposits, mostly in the lower and upper part of the profile. The lowest flood unit is 20 cm in thickness and it is composed of medium to coarse sand with massive structure. An extract of pollen from this unit was dated to $14,090 \pm 100$ ^{14}C yr BP (AA-22452; BC 15,492-14,439). This flood unit is a remnant of the Late Pleistocene flood sequence deposited in this channel

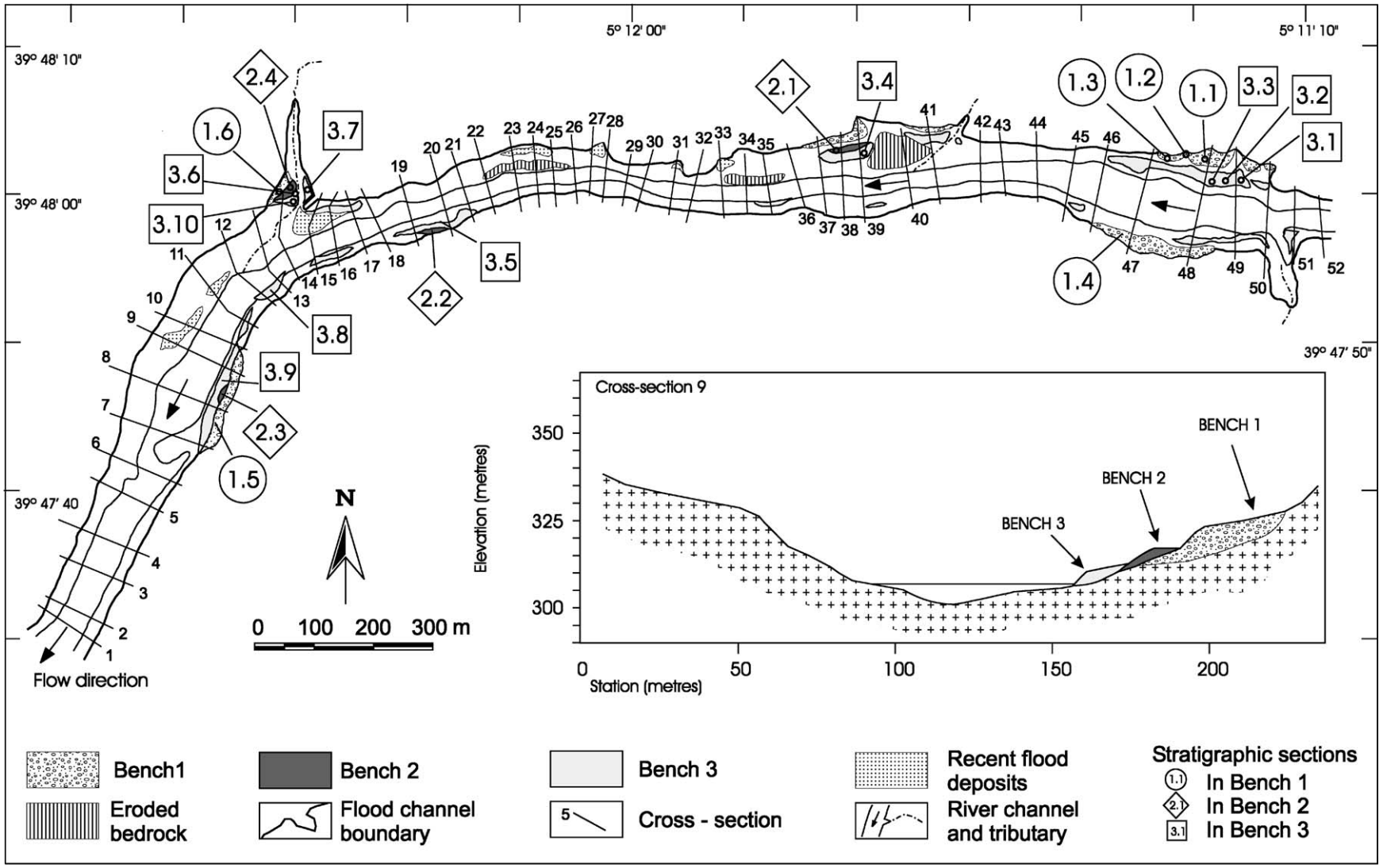

Fig. 2. Location of the slackwater flood deposits along the El Puente del Arzobispo gorge and the stratigraphic sections within Bench 1 (circle), Bench 2 (diamond) and Bench 3 (square). Inset: cross-section 9 shows the stepped bench morphology of the flood deposits and the channel cutting the granite bedrock.

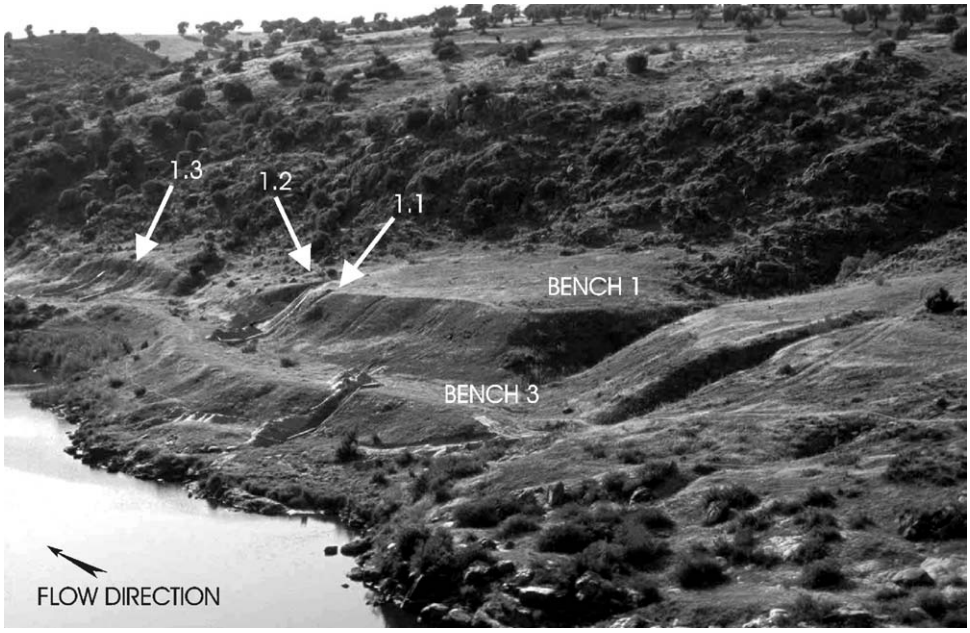

Fig. 3. Downstream view of El Puente del Arzobispo gorge and flood deposits forming Bench 1 and Bench 3 at an expansion reach. The arrows show the location of stratigraphic sections 1.1, 1.2 and 1.3.

Table 1
Numerical dates

Lab No.	Profile No.	Sample No.	Material dated	Flood unit	Analysis	Age (yr B.P.) $\pm 1\sigma$	Calibrated age (1σ)[a]
El Puente delArzobispo							
AA-22452	1.1	TA-53	Po	1	AMS	14,090±100	BC 15,492–14,439
Beta-098317	1.1	28.F8	O	7	AMS	8040±30	BC 7025–7000
GrA-3000	1.2	TA-11-2	Ch	12–13	AMS	9310±50	BC 8628–8476
GrA-3177	1.2	TA-12-1	Sg	20	AMS	8300±80	BC 7517–7184
GrA-3178	1.2	TA-12-2	Sg	17	AMS	8490±80	BC 7587–7486
Beta-098317	1.2	TA-13.1	Sm	27	Conv	6740±60	BC 5055–4900
Beta-098314	1.5	24.3	Sm	1	AMS	9440±50	BC 8540–8420
Beta-098315	1.5	24.2	Sm	12	AMS	9210±50	BC 8250–8110
Beta-87423	2.4	TA-6-1	Ch	5	AMS	410±50	AD 1440–1505 AD 1595–1620
MAD-372	3.3		P	1–2	TL	354±47	
MAD-372a	3.3		P	1–2	TL	378±55	
Beta-87421	3.7	TA-4-2	Ch	1	AMS	170±50	AD 1665–1700, 1720–1820, 1855–1860, 1920–1950
GrA-1702	3.7	TA-4-3	Ch	3	AMS	165±50	AD 1664–1697, 1726–1812, 1842–1875, 1918–1950
Beta-87422	3.7	TA-4-8	Ch	8	AMS	150±60	AD 1670–1950
GrA-1679	3.7	TA-4-8	Ch	8	AMS	80±50	AD 1693–1727, 1815–1859, 1860–1920
GrA-1678	3.10	TA-17-2	Ch	5	AMS	110±50	AD 1689–1731, 1811–1901, 1904–1926
Alcántara							
Beta-119758	A.2	ALC-B.3	Ch	4	AMS	990±50	AD 980–1175
Beta-119757	A.2	ALC-B.2	Ch	6	AMS	940±40	AD 1015–1205
Beta-119756	A.2	ALC-B.1	Ch	8	AMS	410±40	AD 1445–1495
Beta-119759	A.4	ALC-E.1	Ch	2–3	AMS	1200±40	AD 785–885

Note: P, pottery; Ch, charcoal; Sg, gastropod shell, Sm Mollusc shell; Po, Pollen extract O, organic sediment; Conv, radiometric standard; AMS, accelerator mass spectrometry; TL, thermoluminiscence. Beta, Beta Analytic Inc., USA; AA, University of Arizona, NSF Arizona AMS Facility, USA;GrA, Centrum voor Isotopen Onderzoek, Rijksuniversiteit Groningen, the Netherlands; MAD, Laboratorio de Geología y Geoquímica, Universidad Autónoma de Madrid, Spain.

[a] Based on Stuiver and Reimer, 1993.

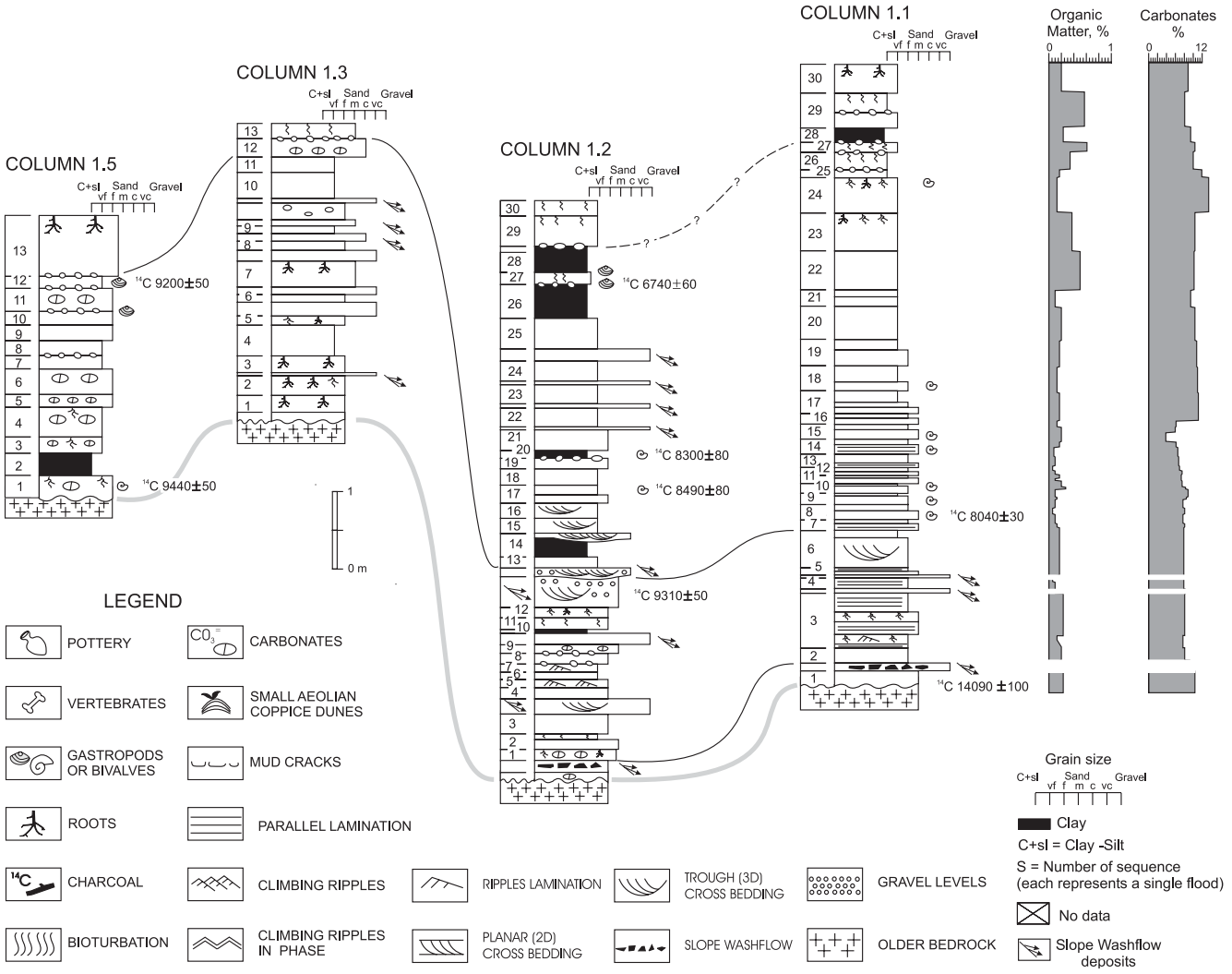

Fig. 4. Stratigraphic sections through Bench 1 (upper bench). Numbers on the left side of the profiles indicate individual flood units/events. Correlations between sections are tentative. The locations of the sections are shown in Fig. 2.

expansion. The unit was eroded by subsequent flood(s) that occurred previous to the deposition of the early Holocene flood sequence. This stratigraphical hiatus is represented in profile 1.1 by a slope deposit layer of 15 cm in thickness and composed of coarse sand and pebble-size grus fragments which overlay the Late Pleistocene flood unit.

The rest of the stratigraphical sequence for profile 1.1 can be separated in four sets. The lower set is overlying the previously described Late Pleistocene flood unit and slope deposit unit, and comprises five flood units (units from 2 to 6, Fig. 4) consisting of sandy textures with a small amount of clay-silt deposits where upwards fining in grain size is common. Current ripples, large-scale trough cross-bedding and parallel lamination are the dominant sedimentary structures. This sequence culminates in a flood unit with high-energy sedimentary structures (large-scale trough cross-bedding), which probably corresponds with a very high-energy flood. Organic matter percentage in these samples is low (0.1–0.2), and carbonate percentage decreases progressively upwards from 10.4 to 7.8. Most of the carbonate is secondary, probably associated with incipient pedogenetic processes, and can be related either to the finer textures that hinder the vertical movement of water or to more arid climatic conditions during the exposure of these flood sediments. Datable material could not be found in this lower set in Section 1.1, although the brown to yellow colour and the extreme consolidation of some flood units are similar to those described in profiles 1.2, 1.3 and 1.5, which have been dated to the early Holocene.

The second set contains 10 successive fine to medium sand graded rhythmites (units from 7 to 16) of 20–30 cm in thickness. Some of these rhythmite couplets show evidence for their deposition by separate flood events, such as a distinct reddish colour and increase of the organic matter of the silt beds. Most of these units are

structureless although parallel lamination, presumably formed as the result of migration of plane beds, may occur in the sand layers. Organic matter varies between 0.1% and 0.2%, and within the couplets the lower medium-sand bed contains higher organic content than the upper bed. Carbonate content varies between 3.8% and 8.8%, usually the lower couplet has a slightly higher percentage and, in the set, progressively the upper rhythmites contain a lower carbonate percentage. A radiocarbon date from charcoal in the second rhythmite (unit 8, column 1.1; Fig. 2) provided an age of 8040 ± 30 ^{14}C yr BP (BC 7025–7000). We may speculate that the other rhythmites were deposited within a short time span or that they may correlate with units 13–17 (column 1.2; Fig. 2) in which radiocarbon dates (by the AMS technique) on terrestrial gastropod shells gave ages of 8490 ± 80 and 8300 ± 80 ^{14}C yr BP (BC 7587–7486 and BC 7517–7184).

The third set shows at least eleven slackwater sedimentation units (units 17–27; Fig. 4), 12–43 cm in thickness, dominated by silty sand and sandy silt textures. Here, stratigraphical breaks are more difficult to determine due to minor changes in texture and massive structure. This set shows a notable increase in the carbonate, which is close to 12% in most of the units. Organic matter in the third set ranges from 0.13% to 0.2%. These units did not contain any datable material. However, in column 1.2, unit 27 includes a river mollusc that was dated to 6740 ± 60 ^{14}C yr BP (BC 5055–4900). The fourth set comprises at least three floods (units from 28 to 30), with a dominant sandy silt texture and massive structure. Most of the flood units were affected by pedogenic processes after deposition, which are reflected in the higher percentages of organic matter (up to 0.6%) and carbonate content (around 10%). These pedogenetic processes may be due to the longer time span between the occurrences of large flood events. In profile 1.1, overlying the uppermost soil, a pale-brown slackwater unit was deposited probably by a historical flood (either AD 1876 or AD 1947).

In the stratigraphical profile 1.1, 62 samples were taken for pollen analysis. Only units 1 and 3 contained pollen, with up to a total of 15 taxons identified (Martín-Arroyo and Ruiz-Zapata, 1996; Martín-Arroyo et al., 1999). These samples showed an important development of arboreal pollen, dominated by *Pinus* and *Quercus-p*, contrasting with the poor content both quantitatively and qualitatively of the herbaceous pollen (Asteroideae, Chenopodiaceae, Lamiaceae, *Plantago* and Poaceae), whilst the shrub pollen is represented by *Juniperus* and Rosaceae. According to Martín-Arroyo et al. (1999), this vegetation represents dry and cold conditions prevailing during the late glacial (pollen content on unit 1, Section 1.1, was dated as $14,090 \pm 100$ ^{14}C yr BP), similar to ones described in other parts of the Iberian Peninsula. Other interesting data obtained by these authors is the presence of quantified percentages of *Castanea* (chestnut tree). Currently, this arboreal taxon is located in humid and temperate zones of the western part of the Iberian Peninsula, and it is likely related to wetter and warmer conditions prevailing during the last deglacial cycle along the Tagus valley.

3.3. Middle bench

Inset within Bench 1, the intermediate deposit (Bench 2) is located 12 m above the channel bottom (Fig. 2). The development of this terrace along the study reach is very poor with a thickness ranging from 1 to 2 m. Its stratigraphy was described in four sites. Bench 2 sections contain between four and six slackwater sedimentation units, dark brown in colour, composed of medium to fine sand and silty sand. Massive beds are dominant although parallel lamination and trough cross-bedding are developed in some of the profiles. Unfortunately, organic material suitable for dating was very scarce. An age reference for this bench was obtained in the slackwater flood deposits accumulated in a tributary mouth (Fig. 5). These flood deposits are overlying the tributary bed and granite bedrock and they are forming two morphological scarps. In these deposits, two trenches 20 m in length were dug from the tributary to the slope, showing two fill insets within the upper bench (Sections 1.6 and 2.4) and a single fill in the lower bench (Section 3.6, Fig. 5). In an equivalent topographical position to the intermediate bench 2, the second infill set is ca 1.5 m in thickness and comprises six flood units, which are composed of silt and fine sand, pale brown in colour, with massive structure. Most contacts between flood units are diffuse. Stone lines, buried soils, and broken root marks were the main criteria for separating different flood events. A charcoal sample collected in a flood unit at the middle part of the profile (unit 5) gave an age of 410 ± 50 ^{14}C yr BP (AD 1445–1495). Assuming that this second infill is also chronologically equivalent to bench 2, the intermediate slackwater terrace of the El Puente del Arzobispo was formed during historical times (15–17th Centuries).

3.4. Lower bench

The lower terrace (Bench 3) developed along the El Puente del Arzobispo gorge, is either inset within Bench 1 (Fig. 3) and Bench 2 or attached directly to the channel margins at bedrock protected sites (Fig. 2). This is the most ubiquitous slackwater terrace developed along the study reach. The top surface of Bench 3 along this study reach is about 10 m above channel bottom. Detailed stratigraphical profiles were described at 7 sites (Fig. 2) where deposits ranged from 2 to 5 m in thickness containing between 7 and 19 slackwater sedimentation units (Figs. 5 and 6). These slackwater

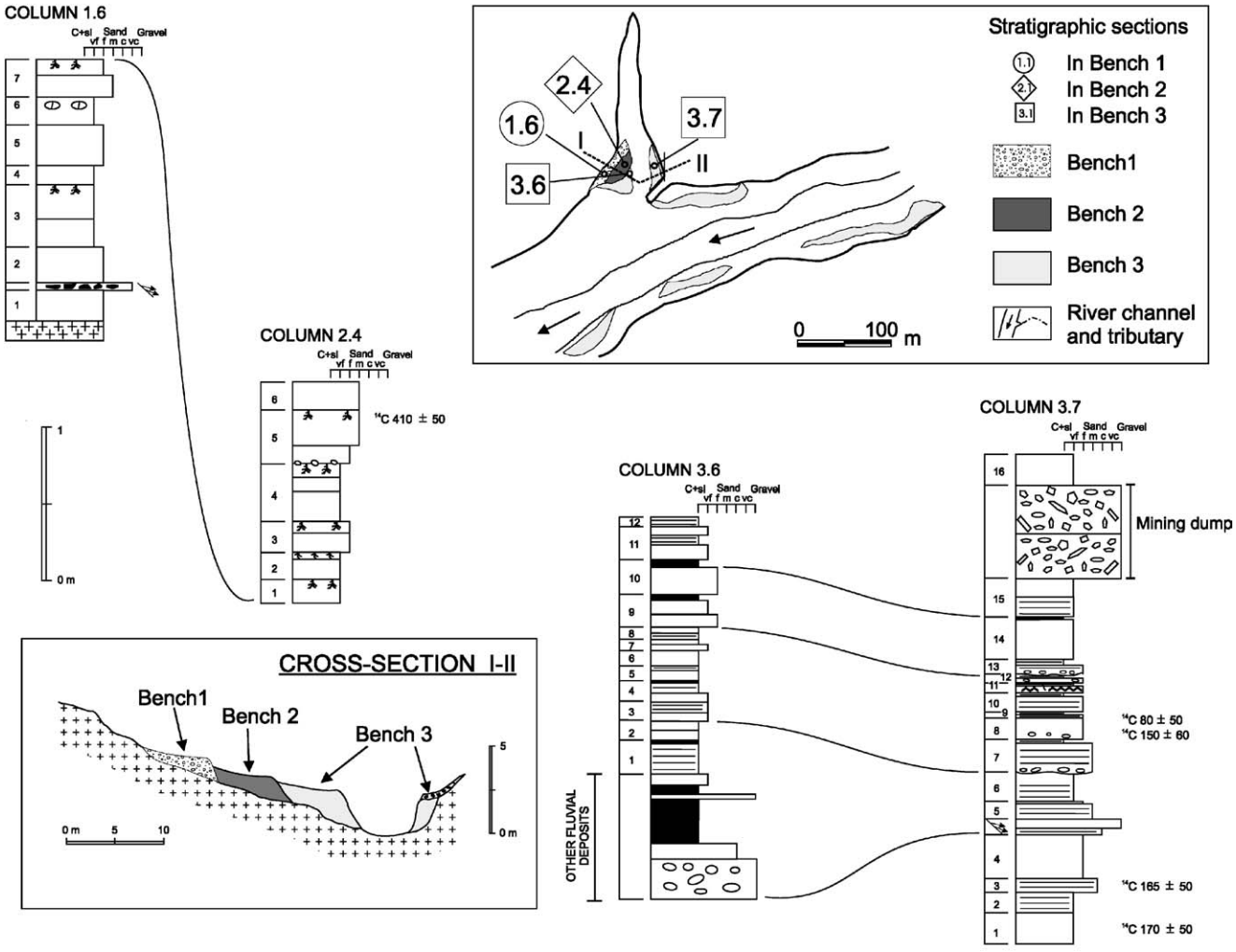

Fig. 5. Stratigraphic sections through the slackwater flood deposits within the mouth of the tributary Arroyo Molino. The legend is shown in Fig. 4. Upper inset: Plan view of the site and location of the stratigraphic sections. Lower inset: Cross-section along the tributary mouth (from I to II; see upper inset for location).

sedimentation units are between 15 and 75 cm in thickness and they fine upwards from coarse sand to silt with decreasing energy conditions. Sedimentary structures range from upper high-energy parallel lamination to large-scale planar or trough cross-bedding, ripple lamination or massive intervals (Fig. 6). Stratigraphical breaks separating individual floods are frequently represented by fine drapes of silt and clay. In site 3.3 (Fig. 6), the slackwater Bench 3 overlies an archaeological site with abundant remains of pottery and bones. Two pottery pieces were dated by a thermally stimulated luminescence (TL) technique as 378 ± 55 and 354 ± 47 yr ago. The archaeological site predates the slackwater sedimentary sequence, although some of these sediments are probably of a much later age (19th and 20th Century). Flood sediments forming Bench 3 along the gorge have a very loose consistency and furthermore, in profile 3.9 with 13 stratigraphical contacts (Fig. 6), the third uppermost flood unit contained an aluminium paper fleck with 88% aluminium oxide content (determined by scanning electron microscopy with energy disperse X-rays) suggesting a maximum age of around AD 1975 for these floods, probably corresponding to the AD 1978 or 1979 floods.

Flood deposits forming the lower bench in the tributary mouth (profiles 3.6 and 3.7; Fig. 5) provided further details on the chronology of Bench 3, although its greater consolidation may indicate an older age. Profiles 3.6 and 3.7 are located on the left and right sides of the tributary mouth (Fig. 5). Profile 3.7 provides evidence of at least 16 floods. Slackwater deposit units are composed of fine sand and silt texture occasionally culminated by thin clay layers (drapes), forming upward fining grain size sequences. Parallel lamination is the dominant sedimentary structure, and rip-up clasts, flaser and lenticular structures, and lines of charcoal flakes can

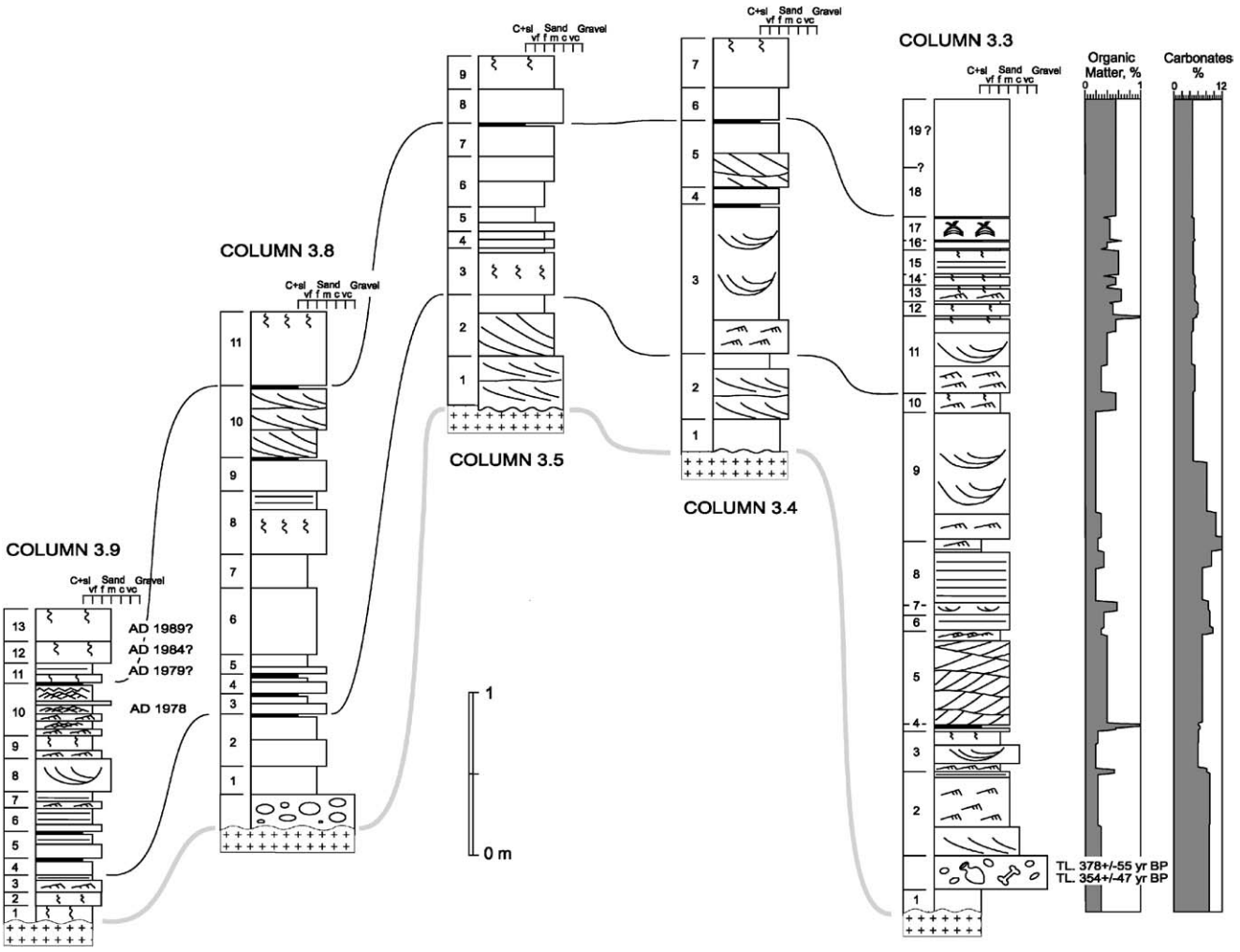

Fig. 6. Stratigraphic sections through Bench 3 (lower bench). The legend is shown in Fig. 4. and location of the sections in Fig. 2. Numbers on the left side of the profiles indicate individual flood units/events. Correlations between sections are tentative.

be observed in some units. Most of the contacts between units are sharp and frequently slightly erosive with clast accumulations at the bottom of the units. Charcoal material from the lower part of the profile indicate absolute ages of 170 ± 50 ^{14}C yr BP (AD 1665–1950) and 165 ± 50 ^{14}C yr BP (AD 1664–1950), and at the middle part deposits were dated as 150 ± 60 ^{14}C yr BP (1670–1950) and 80 ± 50 ^{14}C yr BP (AD 1693–1920). A 50-cm thick accumulation of boulders (23 cm in diameter), gravels and pebbles with chaotic structure at the top of the slackwater units were caused by mining activities located upslope operating at the beginning of the 20th Century. Another profile within the tributary mouth (profile 3.10; Fig. 2) shows five flood units overlying an older flood deposit yellowish in colour. These units are 10–20 cm in thickness, and are composed of silt and fine sand with parallel lamination or massive structure. A charcoal flake collected in the second youngest flood unit in the profile was dated by AMS to 110 ± 50 ^{14}C yr BP (AD 1689–1926).

The pollen study of 15 samples from profile 3.3 showed two groups, which are separated by a middle sterile layers (Martín-Arroyo and Ruiz-Zapata, 1996). In this profile, no major changes in vegetation during the time scale represented on the diagram were detected. *Quercus P.*, *Olea* and *Pinus* are the three principal components of the arboreal pollen, *Juniperus*, Ericaceae and Cistaceae, the shrub pollen, and Cichoroideae and Asteroideae, the herbaceous pollen. Flood unit 1 (profile 3.3) contains up to 60% of arboreal pollen, whereas in flood unit 3 the levels of *Quercus p.* pollen fell below 5%, whilst the herbaceous pollen, namely Cichoriaceae, Poaceae and Chenopodiaceae, increased. In the upper zone (from unit 10 to 19), the same pollen elements were found, although distributed differently and with more shrub pollen, indicating a landscape covered in heath dotted with trees. The vegetation changes indicated by the pollen content can be interpreted as the results of human intervention and for the manufacture of charcoal (Martín-Arroyo and Ruiz-Zapata, 1996).

3.5. Discharge estimation

The discharge estimations associated with the slackwater flood deposits at El Puente del Arzobispo were calculated using the US Army Corps of Engineers River Analysis System computer program-HECRAS (Hydrologic Engineering Center, 1995). The computation procedure is based on the solution of the one-dimensional energy equation, derived from the Bernoulli equation, for steady gradually varied flow. Palaeoflood discharge reconstruction was based on the calculation of the step-backwater profile which best matches geological evidence of the flood stage.

Fifty-four cross-sections about 25 m apart were obtained from field survey using an electronic distance meter (EDM) along a 1500 m reach where the stratigraphical sections are located. The accuracy of the discharge estimations depends on stability of the cross-section geometry through time. In stable, bedrock-confined channels, such as in the studied reaches, channel geometry at maximum stage is known or can be approximated because major changes apparently have not occurred over the last several thousand of years. Here, the step-back water calculations, together with the geologic references of flow stages, provide precise discharge estimates. It was assumed for the calculations that flow was subcritical along the modelled reach. Manning's n values of 0.03 and 0.045 over the valley floor and margins, respectively, were assigned. A sensitivity test performed on the model shows that for a 25% variation in roughness values, an error of 4% was introduced into the discharge results. The selection of the boundary conditions was more critical for the discharge results. Additional cross-sections were obtained from a map 1:5000 in scale in order to set up the appropriate boundary conditions. After running the model along a reach of 25 km in length, critical flow was found in one cross-section that was located 3.5 km downstream of the study reach.

Discharge values associated with each slackwater bench were estimated upon calculated water surface profiles bracketing bench elevations at different sites along the longitudinal profile (Fig. 7). Three discharge values were used to characterise each flood bench (Fig. 7), (1) the base of the flood bench; (2) the top of the scarp of the flood bench; and (3) the highest end point of the flood bench at the contact with the canyon slope. It is apparent that the bench scarp may have been reworked and lowered by slope wash erosion, and therefore, discharge matching the scarp may be considered as conservative. On the other hand, the highest end point of the flood bench, at the contact with the canyon slope is frequently 2.5–3 m higher than the bench scarp. Although some slope accumulation may be present at this inner zone of the flood bench, these end points indicate the maximum emplaced area of the flood

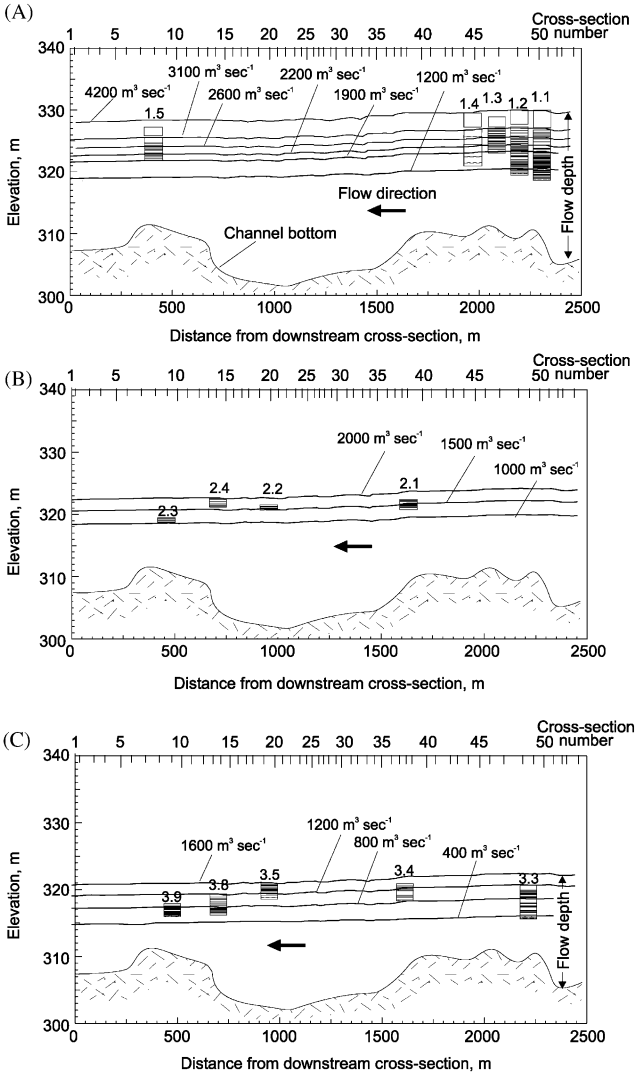

Fig. 7. Calculated step-backwater surface profiles for different discharges along the El Puente del Arzobispo gorge associated with slackwater flood Bench 1 (A), Bench 2 (B) and Bench 3 (C). Stratigraphic sections related to those benches and cross-section locations are shown in Fig. 2.

flow. A similar criteria but applied to individual slackwater flood deposit unit end points, was used by Yang et al. (2000) to provide a better approximation to the flood stage during peak discharge.

On the basis of calculated water-surface profiles along the study reach, the early Holocene flood deposit bench (in Section 1.5 at least 12 events between 9440 ± 50 ^{14}C yr BP and 9210 ± 50 BP ^{14}C yr BP; BC 8540–8110) is associated with minimum estimated discharges of 1900 $m^3 s^{-1}$ (base) 3000 $m^3 s^{-1}$ (scarp) and 4000 $m^3 s^{-1}$ (highest end point) (Fig. 7A; Fig. 8).

The second set of flood units comprising 10 successive fine sand-to-medium sand graded rhythmites in stratigraphic Section 1.1 (one dated as 8040 ± 30 ^{14}C yr BP and the correlated units in Section 1.2 dated as 8490 ± 80

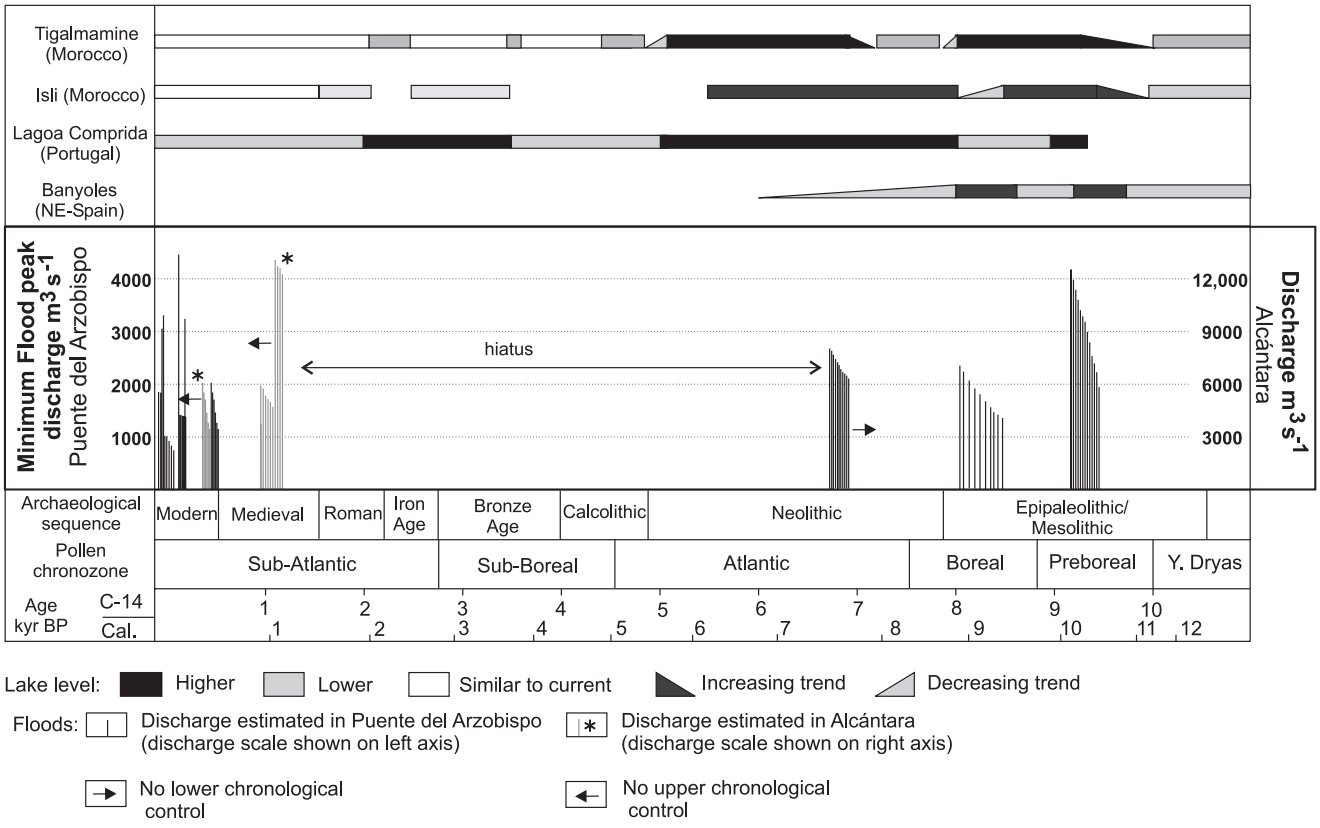

Fig. 8. Palaeoflood temporal distribution and discharge estimates of the Tagus River during the Holocene. Each bar represents a single flood event. In the upper part, lake level changes from selected sites is shown. Lake Levels: Tigalmamine lake (Morocco) after Lamb et al., (1989); Isli lake (Morocco) after Zeroual (1995); Lagoa Comprida (Portugal) after Van der Brink, L.M., Janssen, C.R., (1985); and Banyoles (NE-Spain) after Pérez Obiol and Juliá (1994), Roca and Juliá (1997); Juliá et al. (1998); and Valero-Garcés et al. (1998).

and 8300 ± 80 ^{14}C yr BP; BC 7025–7000, BC 7587–7486 and BC 7517–7184) is associated with minimum discharges between 1200 and 2200 m^3 s^{-1} (Fig. 8). There is no field evidence to provide an upper range of discharge estimates for these flood units. In Sections 1.1 and 1.2 the third fill set (at least 11 flood units) containing a dating at the upper portion of this set of 6740 ± 60 ^{14}C yr BP (BC 5055–4900) matched with discharge estimates between 2200 and 2600 m^3 s^{-1} (Fig. 8). The upper and fourth fill set within Sections 1.1 and 1.2 (at least three flood units) matches with discharge estimates of 2600 m^3 s^{-1} (base), 3100 m^3 s^{-1} (scarp), and 4200 m^3 s^{-1} (end point). Unfortunately, the lack of organic material avoided numerical dating of these flood units which comprise the largest flood that occurred in the Tagus River during the last 4000 yr. Information on historical floods indicate that this palaeoflood record should include the AD 1876 flood and AD 1947 flood, the latter flood having at least reached the bench scarp.

The slackwater Bench 2 comprising between four and six sedimentary units was associated with an estimated minimum discharge of 1000 m^3 s^{-1} (base) to 2000 m^3 s^{-1} (top) (Fig. 7B; Fig. 8). In fact, flood unit five in stratigraphic Section 2.4 and dated as 410 ± 50 ^{14}C yr BP (AD 1445–1495) matches with a water surface profile of 2000 m^3 s^{-1}.

The slackwater Bench 3, comprising upto 19 flood units, has an associated maximum age of 378 ± 55, and includes the most recent floods (AD 1978, 1979, 1984 and 1989). Flood discharges are bracketed by minimum values that range between 400 and 1200 m^3 s^{-1} in Section 3.3 (Fig. 7C). However, flood deposits forming the lower bench in the tributary mouth (profiles 3.6 and 3.7) include at least 16 floods having occurred since AD 1664 and whose minimum discharge magnitudes range between 800 and 1600 m^3 s^{-1}.

The nearest gauge record to El Puente del Arzobispo is that of Talavera de la Reina, approximately 60 km upstream of the study reach. The peak discharge record is incomplete and includes the periods 1942–1949 and 1971–1990. During these periods only two floods exceeded 1500 m^3 s^{-1} and four floods surpassed 1000 m^3 s^{-1}. The largest flood during this instrumental period occurred in March 1947. Reported peak discharge inferred by rating curve extrapolation was 7320 m^3 s^{-1}or approximately four times that of the second largest recorded flood. The field data suggest

that the 1947 discharge values were overestimated. The water surface elevation was documented on marks on the walls of buildings at El Puente del Arzobispo. According to these marks the 1947 flood discharge more likely was between 2500 and 3000 $m^3 s^{-1}$.

Currently, the Tagus River is fully regulated by dams that have inundated most of the channel and floodplain areas downstream of Talavera de la Reina (central part of the basin) to the Portuguese border. The Azutan dam, approximately 15 km upstream of El Puente del Arzobispo was built in 1969 for hydroelectric purposes. The spillway was designed for flood control with a discharge capacity of 6000 $m^3 s^{-1}$. According to our study, the Azutan dam spillway is clearly over dimensioned for any flood that has occurred in the last 10,000 yr.

4. Alcántara

Alcántara reach is located 10 km upstream of the Portuguese border, and ca 170 km downstream from El Puente del Arzobispo, covering a catchment area of 51,958 km^2. Here, the Tagus River flows through a 500 m-wide constricted segment incised ca 150 m into schist and slates. The physiography of the Tagus River valley is characterised by steep slopes and development of rock-cut terraces in which the river has cut a 100 m wide low-flow channel. In the study reach, water is regulated by the Cedillo dam, built in 1975, and located ca 50 km downstream. The reservoir water level constrains the potential location of the slackwater sites.

4.1. Flood geomorphology and stratigraphy

In the Alcántara gorge, recent flood deposits mantle the rock-cut terraces (Fig. 9). Erosional and depositional evidence of high-magnitude flood stages is ubiquitous along the gorge. The most abundant erosional features are scoured surfaces carved on the bedrock sidewalls of the gorge. In some reaches, distinct scour lines etched into the hillslope, below which floods have removed unconsolidated slope deposits that formerly overlaid the bedrock. The slackwater flood deposits occur as (1) narrow benches parallel to the river valley (site A.4; Fig. 9), (2) benches at the tributary mouths (sites A.1 to A.3; Figs. 9 and 10) and (3) benches in the tributary valleys several hundred metres upstream from the tributary junction (profile A.5 in Fig. 9).

In the main valley, high-level flood deposits form narrow benches. Some of then are only visible by on-site observation. The thickness of these deposits varies from 1 to > 5 m. A trench dug in a high bench (profile A.4; Figs. 9 and 11) shows at least four flood units composed of medium to fine sand and silt beds with dominantly massive structure. Contacts between units are clearly

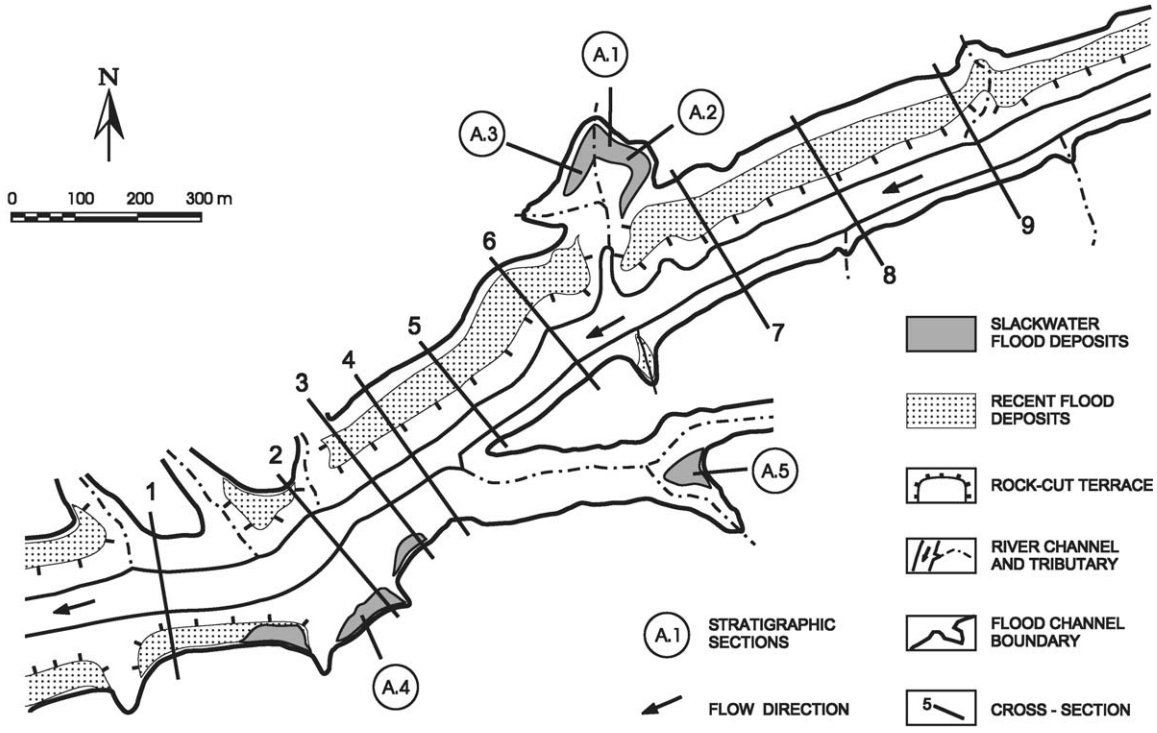

Fig. 9. Location of the slackwater flood deposits along the Alcántara gorge and the stratigraphic sections A.1, A.2, A.3 described in Fig. 11. The cross-sections were used for the hydraulic calculations.

delineated by colour and textural changes, wash-slope material on top of the units, truncated bioturbation and root marks. Charcoal found in a slope deposit in the middle part of the stratigraphical profile was dated as 1200 ± 40 ^{14}C yr BP (AD 785–885), indicating that at least three extremely large floods have occurred since the ninth century.

The most prominent flood deposits are located in the tributary valleys, both in the tributary mouth and in the upstream part of the valleys, which are backflooded during Tagus River floods. The most spectacular deposition occurred at the confluence of two tributary streams ca 200 m from the main Tagus River channel (Fig. 10). The geometry of this setting is perfect for the deposition of slackwater deposits. In the first 100 m, near the confluence, the tributary channel flows through a constricted reach closely bounded by stepped cliffs, opening up in the following 100 m reach with an amphitheatre-like shape (Figs. 9 and 10). During floods, this very low energy backflooded environment favours deposition of very fine and fine sand, silt and even clay sediments. The study of these slackwater flood deposits is complicated because the flood units are not stacked horizontally and they do not form vertical arranged benches, such as in the El Puente del Arzobispo. Here, a rounded-mound of flood deposits attached to the valley slope was formed by the semiconcentric accretion of successive layered flood deposits. Several trenches were dug by hand at different parts of the 21 m-high flood deposits in order to obtain the most complete stratigraphy possible. The best profile (A.2) (Fig. 11) shows at least 16 flood units with subtle contacts between flood units. Flood units range from 6 to 45 cm in thickness and are composed of fining-upward sequences formed by the combination of one or more of the following subunits: very fine sand with parallel lamination, structureless silt, and clay textures affected by cracks. High bioturbation due to roots, annelids and arthropods is ubiquitous throughout the stratigraphical profile. The lower part of the profile was bracketed by radiocarbon ages of 990 ± 50 ^{14}C yr BP (flood unit 4; AD 980–1175) and 940 ± 40 ^{14}C yr BP (flood unit 6; AD 1015–1205), and in the middle part a charcoal sample was dated as 410 ± 40 ^{14}C yr BP (flood unit 8; AD 1445–1495). In a 1.8 m thick section located near the slope (profile A.1), at least four flood units (8–26 cm in thickness) were described, which are composed of silt and clay textures with very thin parallel lamination frequently affected by bioturbation due to annelids and arthropods. These fine-grained flood deposits are separated in some units by 15–50 cm thick colluvial units composed of sand and scattered pebble-sized

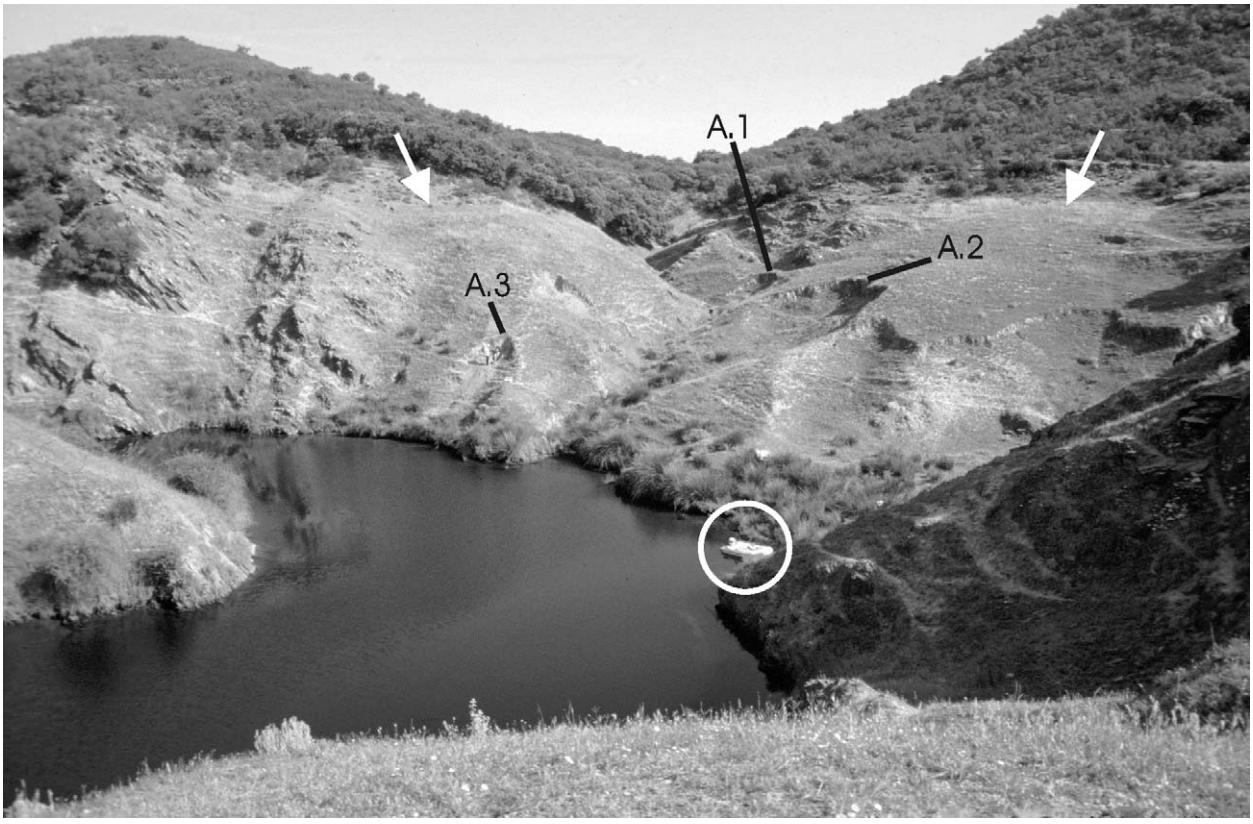

Fig. 10. Uptributary view of the slackwater flood deposits at Alcántara. Arrows show the uppermost part of flood deposits which correspond to minimum peak discharges of 11,000 m^3 s^{-1}. A boat, 4 m in length, is circle for scale.

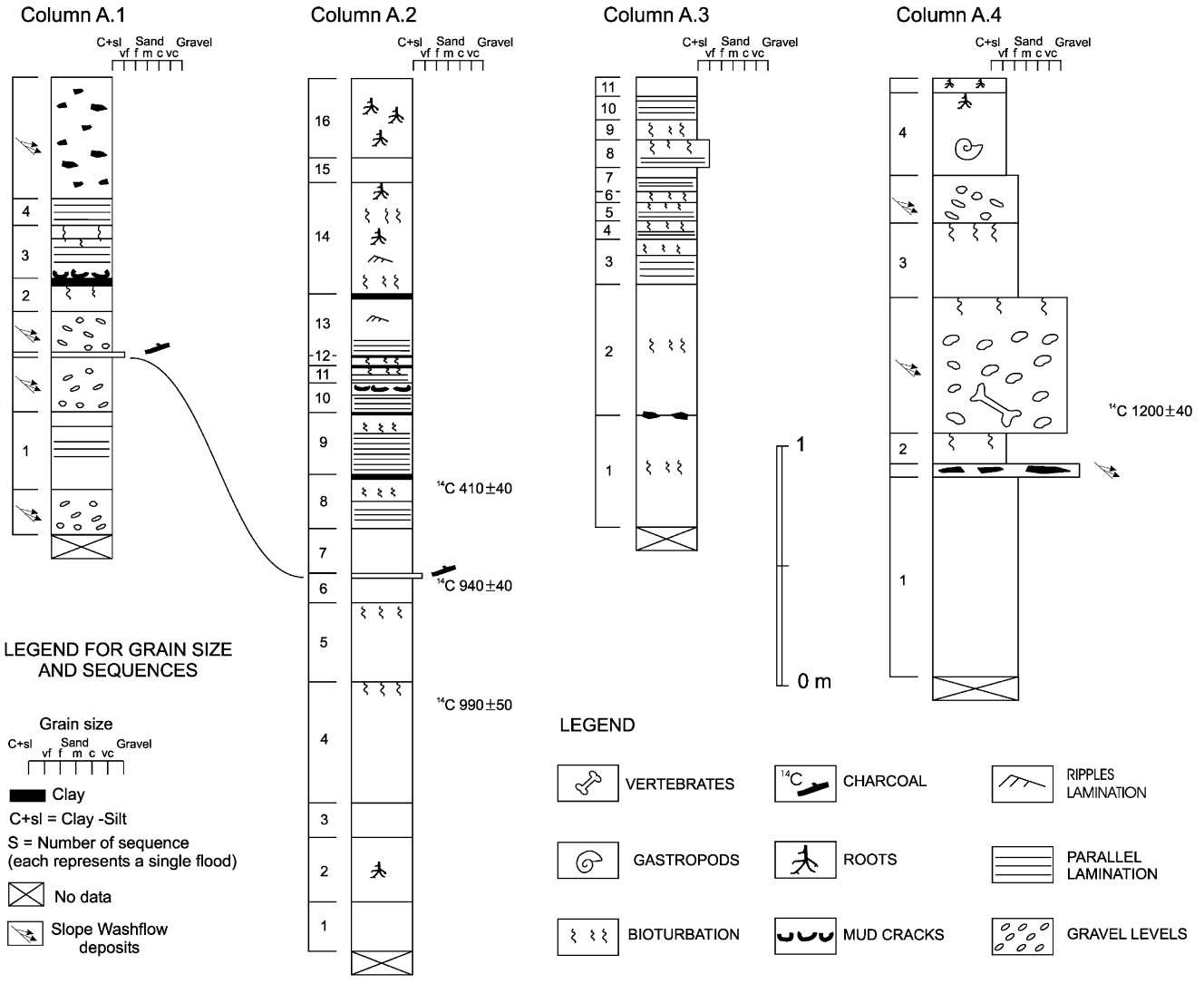

Fig. 11. Stratigraphic sections of the slackwater flood deposits in the Alcántara gorge. Numbers on the left side of the profiles indicate individual flood units/events. The location of the sections are illustrated in Fig. 9.

fragments. Datable material was not found in the section.

4.2. Discharge estimation

Ten cross-sections along a reach of 1400 m in length were obtained by field survey using an EDM surveyor and an echosounder. These cross-sections were then used in the HEC-RAS model to estimate palaeoflood discharges that were assumed to have involved sub-critical hydraulic flow. In order to reduce uncertainties during the selection of the boundary conditions for downstream cross-sections, 23 additional cross-sections were measured from topographic maps 1:5000 in scale (5 m contour intervals) along a reach of 5 km downstream of the surveyed cross-sections. Discharges were estimated for Manning's n values between 0.03 over the valley floor and 0.04 over the margins. For a 15% variation in roughness value, an error of 3–5% was introduced in the discharge results. Uncertainties of up to 15% on the discharge results were introduced by the boundary conditions selected for the steady flow modelling in the initial cross-section (most downstream cross-section for subcritical flow). The model was run assuming critical flow conditions on the first cross-section located in the entrance to an extremely narrow reach 5 km downstream of the studied reach. However, it is possible that the hydraulic control section can be located farther downstream within the Portuguese part of the Tagus River.

On the basis of calculated water-surface profiles along the study reach, the highest elevation for geological evidence of former floods (located in cross-section 9) is associated with a minimum discharge of $15,000\ m^3\ s^{-1}$. The step-backwater calculations show a minimum peak discharge for profile A.4 (cross-section 4; water depth of

30 m) of 12,000 m^3 s^{-1}, indicating that at least 3–4 floods over this magnitude occurred after AD 785–885. Other narrow flood deposit benches along the gorge provided minimum discharges of 13,700 m^3 s^{-1} (cross-section 7), 11,200 m^3 s^{-1} (cross-section 6), and 10,100 m^3 s^{-1} (cross-section 5). The location of these flood deposits along straight reaches of the gorge, and attached to its margins, is not the optimum for sediment preservation. Therefore, these deposits attached to the gorge margins are expected to be periodically flushed out by very extreme floods (occupying these margins as effective flow areas) and replaced by sediments left by smaller magnitude floods. These flood erosional–depositional dynamics may explain the limited stratigraphy and the short-time framework covered by the flood deposits at Alcántara, compared to the long flood record found in the channel expansion environments of El Puente del Arzobispo where erosion by extreme floods is less likely.

During large floods, the rise in water stage of 30–36 m, as evidenced by the flood deposits, produced extensive backflooding of the tributaries affecting areas several hundred metres upstream of their junctions with the Tagus River. In these backflooded environments, the slackwater conditions favour deposition of relatively complete flood histories such as in sites A.1 to A.3 (Figs. 9 and 11). Here, the highest part of the slackwater sediments matches a water surface profile of 11,000 m^3 s^{-1} (cross-section 8). Stratigraphic section A.2, comprising at least 16 flood units, is associated with minimum discharges of 4100 to 6000 m^3 s^{-1} , with at least four floods occurring after AD 980–1175, two floods after AD 1015–1205, and nine floods after AD 1445–1495. In the same tributary, Section A.1, with at least four flood units, and Section A.3 with at least 11 flood units, are associated with minimum discharges of 5600 and 3400 m^3 s^{-1}, respectively.

The past flood record in this reach can be supplemented using evidence associated with landmarks and documents connected with the Alcántara Roman bridge, located ca 6 km upstream of the study reach. This bridge is an impressive civil engineering work built in AD 103. The bridge is ca 200 m in length and 7 m in width with two central arches having respective openings of 28.8 and 27.4 m in height, and supported by two lateral arches with openings of 21.9 and 13.8 m in height. In Alcántara, the largest floods during the last 200 years were recorded in AD 1876, 1941, 1947 and 1856 in which the exact water stages are known. Application of these stages in the HEC-RAS model provides peak discharge estimates of 14,800, 13,700, 11,800 and 10,500 m^3 s^{-1}, respectively (Benito et al., 2003b). The HEC-RAS modelling was calibrated for the 1989 and 1996 floods, using discharge data recorded in the Alcántara dam and the water stages recorded in photos and videos at different times. Other important floods occurred in 1912 and 1989 when estimated respective peak discharges were 3800 and 7500 m^3 s^{-1}.

We estimate that elevations for the highest flood deposits represent minimum discharges approximated at about 15,000 m^3 s^{-1}, and were produced by the AD 1876 flood and/or floods of similar magnitude. Section A.4, with minimum discharge estimate of 12,000 m^3 s^{-1}, may contain deposits from the AD 1876 and 1941 floods. At least two more floods of this magnitude occurred since AD 785–885 according to the stratigraphic record. Since AD 1856, at least five floods exceeded 6000 m^3 s^{-1}, which are probably included in the upper part of Section A.2 where nine events postdated AD 1445–1495. It is also possible that the number of floods exceeding 6000 m^3 s^{-1} of discharge for the last 500 yr is greater than nine, but field exposures (after digging) were not complete enough to obtain a complete stratigraphic record.

5. Discussion

Slackwater flood deposits along the Tagus River provide an excellent record of more than 80 floods that have occurred during the last 10,000 yr. The palaeoflood record shows that extreme floods are not randomly spaced in time but tend to cluster during specific periods (Fig. 8). High-magnitude floods occurred on the Tagus River from 9440 to 9210 ^{14}C yr BP (8540–8110 BC), 8500 to 8000 ^{14}C yr BP (7500–7000 BC), ~6750 ^{14}C yr BP (~5000 BC; based on one date only), 1200 to 950 ^{14}C yr BP (AD 785–1205), ~410 ^{14}C yr BP (AD 1450–1500, based on two dates), and 170 to 80 ^{14}C yr BP (AD 1670–1950). The largest flood(s) occurred from 9440 to 9210 ^{14}C yr BP, ~6750 ^{14}C yr BP and 1200 to 950 ^{14}C yr BP when minimum discharges during these periods are estimated to lie between 4000 and 4100 m^3 s^{-1} in the El Puente del Arzobispo reach (central part of the catchment; 35,000 km^2 in drainage area) and between 13,700 and 15,000 m^3 s^{-1} in the Alcántara reach (lower part of the catchment, 52,000 km^2 in drainage area). In contrast, the periods 9210–8500 ^{14}C yr BP (8110–7500 BC), 8000–6750 ^{14}C yr BP (7000–5000 BC), and 950 to 410 ^{14}C yr BP (AD 1205–1450) are characterised by relatively few large floods. Periods with few or no palaeoflood deposits do not necessarily indicate a total absence of floods, but are probably times of lower magnitude, moderate floods that did not exceed the threshold of preservation in the depositional sites (Ely, 1997). However, due to the possibility of post-flood erosion, the lack of dating between 6750 ^{14}C yr BP and 1200 ^{14}C yr BP (5000 BC to AD 778) cannot be interpreted as a lack of occurrence of large floods during this period in the present study area.

Most of the precipitation and flooding in large Iberian river basins, such as the Tagus River, is associated with

zonal flow lying between 35° and 45°N. General features of present-day atmospheric circulation were probably in existence by the mid- to late Holocene (Knox, 1983). Since flooding is an important source of water to natural systems, especially in the Iberian Peninsula, periods with a higher frequency and/or magnitude of floods usually coincide with other indicators of climate/environmental change, such as pollen and lake level records.

Late Pleistocene and early Holocene atmospheric circulation patterns were affected by changes leading to combinations of dry/wet and cool/warm conditions since the Last Glacial Maximum (LGM). During the Younger Dryas (about 8°C cooler than today), the large-scale atmospheric circulation regime was characterised by the predominance of a high-pressure cell at middle latitudes, which displaced storm tracks into very low latitudes (Lamb, 1971). In northwestern Spain (Allen et al., 1996), pollen-based palaeoclimatic reconstructions indicate a dry and cool climate with strong seasonality from 14,600 to 12,400 ^{14}C yr BP and during the Younger Dryas (10,700–9800 ^{14}C yr BP). Lake levels during the Younger Dryas period were very low in the Iberian Peninsula, with pollen assemblages characterised by mesic trees indicating a cold and dry climate (Peñalba et al., 1997; Roca and Juliá, 1997; Valero-Garcés and Kelts, 1997; Juliá et al., 1998; Wansard et al., 1998). These cold and dry conditions could also affect the flood frequency over the Iberian Atlantic basins, and it may explain the lack of palaeoflood record in the Tagus River during this period.

The climatic changes experienced immediately after the Younger Dryas period are well represented in the palaeoflood record with an anomalous number of very large floods, at least 12 floods in ~400 yr, from 9440 to 9210 ^{14}C yr BP (BC 8540 to 8110; Fig. 8). Because of the large size of the river catchment (ca 35,000 and 52,000 km^2), years with occurrence of extreme floods are usually related to anomalously wetter conditions. This flood period can be interpreted as related to westerly dominated hemispheric circulation with the Azores High at lower latitudes and a low index zonal circulation over the Atlantic. In Banyoles and Salines lakes in NE Spain, periods of increased rainfall and water balance have been correlated with the Bølling-Allerød and Preboreal periods (Roca and Juliá, 1997; Juliá et al., 1998; Valero-Garcés et al., 1998; Wansard et al., 1998). Lake level record and pollen analysis of Laguna Comprida (Serra de Estrela, Portugal) showed wetter conditions in the Preboreal suggesting an increase in winter precipitation in the Atlantic side of the Iberian Peninsula (Van der Brink and Janssen, 1985; Van der Knaap and van Leeuwen, 1995).

The clusters of moderate floods from 8500 to 8000 ^{14}C yr BP (BC 7600–7000) coincide with high lake level and forest development in the Iberian Peninsula and Morocco (Fig. 8). In the Tigalmamine Lake, in the Middle Atlas, Lamb et al. (1989) describe a marked environmental change due to increased available moisture at about 8500 yr ^{14}C BP, interpreted from lake water level rise, isotopic evidence for climatic change, and a rise in the percentage of cedar pollen. In Morocco, precipitation patterns are also associated with frontal systems entering from the Atlantic, although the persistence and intensity of these patterns depends on the latitudinal location of the zonal flow. A pollen record from Padul in southeast Spain, showed an expansion of sclerophyllous oak forest towards 8000 ^{14}C yr BP which marks the onset of the hot and humid Holocene optimum (Pons and Reille, 1988).

Unfortunately, the poor chronological control of the middle and late Holocene palaeoflood record prevents inferences to be made regarding the responses of floods to climate change for some periods. One flood unit dated as 6740 ^{14}C yr BP (BC 5055–4900) is not enough to indicate a flood period at that time. At a global scale, the most prominent Holocene climatic event recognised in the Greenland ice-core climate proxies, with approximately half the amplitude of the Younger Dryas, occurred ca 7500 ^{14}C yr BP (8000–8400 calendar years BP; Alley et al., 1997). There is no evidence of extreme floods during these dry periods in the Tagus River.

One of the most important changes in the pattern of the Mediterranean and North African climatic circulation was recorded at 4000 BP, although the effects of these changes varied with the region. In the Middle Atlas, Lamb et al. (1989) interpreted the arrival of cedar at 4000 ^{14}C yr BP as indicating an increase in moisture, whereas palynological records from Tunisia (Ritchie, 1984), SE-Spain (Pons and Reille, 1988), and southern Europe (Huntley and Birks, 1983) have been interpreted as a return to dry conditions. These dry conditions seem to prevail throughout the late Holocene in the Ebro valley (Davis, 1994; Valero-Garcés et al., 2000). Another change affecting the late Holocene palaeohydrology is the extensive deforestation produced after 2500 yr BP (Burjachs et al., 1997; Ruiz-Zapata, 1999). This vegetation change may affect the flood peak hydrograph with an increase in the peak discharges, although flood occurrence would be still controlled by the persistence of the frontal systems over the Peninsula and by the amount of the rainfall. Indeed, there is evidence of large floods during the last 3000 yr reaching peak discharges of similar order of magnitude to the Preboreal floods, although the chronological limitations do not allow for further precision until the last 1500 yr.

The frequency and magnitude of floods increased again between 1200 and 950 ^{14}C yr BP (AD 785–1205; Fig. 8). This palaeoflood evidence is corroborated by documentary sources of historical floods, especially between AD 1150 and 1200 (Benito et al., 1996, 2003b). A sharp decrease in the frequency and

magnitude of palaeofloods from 950–410 ^{14}C yr BP (AD 1205–1450) may have some relationship to the climatic signals prevailing in the western Mediterranean at the end of the Medieval Warm Period, although the onset and termination of this period is still in debate (Hughes and Díaz, 1994).

For the last 500 yr, the palaeoflood record shows an increase in frequency between AD 1650 and 1900 (170 and 80 ^{14}C yr BP). This increase coincides with glacial advances, high lake levels, and cooler and/or wetter conditions at many sites around the globe during some decades or all of the Little Ice Age (15th to mid-19th centuries; Porter, 1986, Grove, 1988). During the 15–16th centuries, increases in lake levels and general water table rise in the central Ebro valley have be interpreted as the result of increased precipitation and lower evaporation (Valero-Garcés et al., 2000), probably related to the climatic conditions that prevailed during some periods of the Little Ice Age. Palaeoflood chronologies and historical flood records indicate an anomalous concentration of floods during the second half of the 19th century and first-half of the 20th century, a period that also contains the largest floods during the last 750 yr.

Long-term palaeoflood records using slackwater flood deposits are not available in Europe. In Central Europe, phases of a higher flood frequency are found from overbank flood deposit records at about 8500–7700, 6500–6000, 5200–4400, 3000–2600, 2200–1800, 1000 and 400–100 yr BP (Starkel, 1991). The timing of at least three of these periods roughly coincides with those of this study. In the Negev Desert of Israel, Greenbaum et al. (2000) identified in a palaeoflood record two periods of higher frequency of large floods (1380–880 yr BP and the last 60 yr) correlated with high Dead Sea levels and wetter climate conditions, and two periods with low flood frequency (1730–1380 yr BP and 880–60 yr BP), which were correlated to low Dead Sea levels and may be linked to a drier climate conditions. Although these patterns are also found in the studied sites, a higher variability in the flood clusters is recorded in the Tagus River palaeoflood and historical flood records probably due to the type of flood-generating events.

Several analyses of late Holocene flood chronologies have been undertaken in the semiarid southwestern United States (Ely and Baker, 1985; Webb et al., 1988; Enzel, 1992; Ely et al., 1993; O'Connor et al., 1994; Ely, 1997) and in the Upper Mississippi Valley (Knox, 1985, 1993, 1999). Most of the southwestern United States chronologies have been reconstructed from slackwater flood deposits. In a regional synthesis, Ely (1997) observed that the frequency of large floods increased throughout the region from 5000 to 3600 ^{14}C yr BP (3800–2200 BC) and increased again after 2200 ^{14}C yr BP (400 BC) with a maximum in magnitude and frequency of around AD 900–1100, and after AD 1400. In the SW United States, most of the severe current floods are associated with winter storms and tropical cyclones, and these are the most probable causes of the palaeofloods over the last 5000 yr (Ely et al., 1993; Ely, 1997). Despite the differences in the flood-producing storms and geographical settings, the latter two periods (AD 900–1100 and AD 1400) are coincident with the most recent palaeoflood periods recorded in the Tagus River. In the Upper Mississippi Valley and using an excellent record of overbank flood deposits, Knox (1993) describes periods of small floods from 5000 to 3300 cal yr BP (3050–1350 BC), and periods of average increased flood magnitudes after 3300 cal yr BP, and even larger floods from AD 1250 to 1450 at the end of the Medieval Warm Period. Comparison of these flood periods with the Tagus river record is difficult due to the lack of chronologies between 6000 and 1500 yr BP. In the case of the AD 1250–1450 flood period the flood signal is opposite from the pattern found in the Tagus River, where there is no evidence of a large number of exceptional floods.

6. Conclusions

The palaeoflood record of the Tagus River during the Late Pleistocene and Holocene shows non-random occurrence of large floods whose recurrence frequencies appear to be associated with regional climatic/environmental changes as interpreted from lake level variations and pollen records. The largest flood(s) occurred from 9440 to 9210 ^{14}C yr BP (BC 8540–8110), ~6750 ^{14}C yr BP (BC 5000) and 1200 to 950 ^{14}C yr BP (785–1205) and reached estimated minimum discharge magnitudes of between 4000 and 4100 m^3 s^{-1} in the El Puente del Arzobispo reach (Central part of the catchment; 35,000 km^2 in drainage area) and 13,700–15,000 m^3 s^{-1} in the Alcántara reach (lower part of the catchment, 52,000 km^2 in drainage area). High frequency-lower magnitude floods were recorded in the Tagus River from 8500 to 8000 ^{14}C yr BP (7500–7000 BC), ~410 ^{14}C yr BP (AD 1450–1500), 170 to 80 ^{14}C yr BP (AD 1670–1950). The largest floods in the last 750 yr occurred during the second-half of the 19th century and first-half of the 20th century. In contrast, the periods 9210–8500 ^{14}C yr BP (8110–7500 BC), 8000–6750 ^{14}C yr BP (7000–5000 BC), and 950–410 ^{14}C yr BP (AD 1205–1450) are characterised by decreases in the record of large floods.

These periods with increased flood magnitude and/or frequency in the Tagus River are strongly related to increased moisture influx and winter precipitation in the Iberian Peninsula. Proxy records sensitive to winter precipitation such as lake levels and vegetation (through pollen records) are in good agreement with the clusters of floods found in the Tagus River, although floods may

respond faster to a change in rainfall than lake levels or vegetation.

Tagus River palaeoflood periods coincide with some flood clusters found in various regions of the globe such as central Europe, Israel and SW United States, or with low flood frequency periods of regions such as the upper Mississippi valley. This suggests that alterations in the global-scale climate system produce changes in flood regime although signals in terms of magnitude and frequency may vary between regions (Knox, 1993, 2000; Ely, 1997). Further palaeoflood studies and more detailed palaeoflood chronologies are required to provide an important source of information on the immediate hydrological response, at the event scale, to global changes in the atmospheric circulation patterns.

Acknowledgements

This research was supported by the Spanish Committee for Science and Technology (CICYT) grant HID99-0850, FEDER Project 1FD97-2110-CO2-02, and by de European Commission (DG XII), through research contract number EVG1-CT-1999-00010 (Systematic, Palaeoflood and Historical data for the improvEment of flood Risk Estimation, "SPHERE" Project). We wish to thank Tomas Martín-Arroyo and Blanca Ruíz-Zapata for the pollen analysis, to David Uribelarrea del Val, Mayte Rico, Alfonso Benito Calvo, María Fernández de Villalta, and Satur de Alba for their help in the field and to Varyl R. Thorndycraft for his help with the English. Helpful manuscript reviews were provided by Jim Knox, Pete Coxon and Jim Rose.

References

Allen, J.R., Huntley, B., Watts, W.A., 1996. The vegetation and climate of north-west Iberia over the last 14,000 yr. Journal of Quaternary Science 11, 125–147.

Alley, R.B., Mayewski, P.A., Sowers, T., Stuiver, M., Taylor, K.C., Clark, P.U., 1997. Holocene climatic instability: a prominent, widespread event 8200 yr ago. Geology 25, 483–486.

Baker, V.R., 1973. Paleohydrology and sedimentology of Lake Missoula flooding in eastern Washington, Geological Society of America. Special Paper 144, 79pp.

Baker, V.R., 1987. Paleloflood hydrology and extraordinary flood events. Journal of Hydrology 96, 79–99.

Baker, V.R., 1989. Magnitude and frequency of paleofloods. In: Beven, K., Carling, P. (Eds.), Floods: Hydrological, Sedimentological, and Geomorphological Implications. Wiley, Chichester, pp. 171–183.

Baker, V.R., Kochel, R.C., Patton, P.C., Pickup, G., 1983. Palaeohydrologic analysis of Holocene flood slack-water sediment. Special Publication of the International Association of Sedimentologists 6, 229–239.

Barriendos, M., Martín-Vide, J., 1998. Secular climatic oscillations as indicated by catastrophic floods in the Spanish Mediterranean Coastal Area (14–19th Centuries). Climatic Change 38, 473–491.

Benito, G., Machado, M.J., Pérez-González, A., 1996. Climate change and flood sensitivity in Spain. In: Branson, J., Brown, A.G., Gregory, K.J. (Eds.), Global Continental Changes: The Context of Palaeohydrology. Geological Society of London Special Publication No. 115, pp. 85–98.

Benito, G., Machado, M.J., Pérez-González, A., Sopeña, A., 1998. Palaeoflood hydrology of the Tagus River, Central Spain. In: Benito, G., Baker, V.R., Gregory, K.J. (Eds.), Palaeohydrology and Environmental Change. Wiley, London, pp. 317–333.

Benito, G., Sánchez-Moya, Y., Sopeña, A., 2003a. Sedimentology of high-stage flood deposits of the Tagus River, Central Spain. Sedimentary Geology 157, 107–132.

Benito, G., Díez-Herrero, A., Fernández de Villalta, M., 2003b. Magnitude and frequency of flooding in the Tagus Basin (Central Spain) over the last millennium. Climatic Change 58, 171–192.

Bretz, J.H., 1929. Valley deposits immediately east of the Channeled Scabland of Washington. Journal of Geology 37, 393–427, 505–541.

Burjachs-Casas, F., Guiralt, S., Roca, J.R., Seret, G., Juliá, R., 1997. Palinología Holocénica y Desertización en el Mediterráneo Occidental. In: Ibáñez, J.J., Valero-Garcés, B.L., Machado, C. (Eds.), El paisaje mediterráneo a través del espacio y del tiempo. Implicaciones en la desertificación. Geoforma Ediciones, Logroño, pp. 379–394.

Capel, J., 1981. Los Climas de España. Col. Ciencias Geográficas. Oikos-Tau, Barcelona, 429pp.

Davis, B.A.S., 1994. Paleolimnology and Holocene environmental change from endorheic lakes in the Ebro Basin, north-east Spain. Ph.D. Thesis, University of Newcastle Upon Tyne, 317pp.

Ely, L.L., 1997. Response of extreme floods in the southwestern United States to climatic variations in the late Holocene. Geomorphology 19, 175–201.

Ely, L.L., Baker, V.R., 1985. Reconstructing Paleoflood hydrology with Slackwater deposits: Verde River, Arizona. Physical Geography 6, 103–126.

Ely, L.L., Enzel, Y., Baker, V.R., Cayan, D.R., 1993. A 5000-year record of extreme floods and climate change in the southwestern United States. Science 262, 410–412.

Enzel, Y., 1992. Flood frequency of the Mojave River and the formation of late Holocene playa lakes, southern California, USA. Holocene 2, 11–18.

Greenbaum, N., Schick, A.P., Baker, V.R., 2000. The palaeoflood record of a Hyperarid catchment, Nahal Zin, Negev Desert, Israel. Earth Surface Processes and Landforms 25, 951–971.

Grove, J.M., 1988. The Little Ice Age. Routledge, London.

Hirschboeck, K.K., 1991. Climate and floods. US Geological Survey Water Supply Paper 2375, pp. 67–88.

House, P.K., Pearthree, P.A., Klawon, J.E., 2002. Historical flood and paleoflood chronology of the lower Verde River, Arizona: stratigraphical evidence and related uncertainties. In: House, P.K., Webb, R.H., Baker, V.R., Levish, D.R. (Eds.), Ancient Floods, Modern Hazards: Principles and Applications of Paleoflood Hydrology. Water Science and Application 5, American Geophysical Union, Washington DC, pp. 267–293.

Hughes, K.M., Díaz, H.F., 1994. Was there a medieval warm period, and if so, where and when? In: Hughes, M.K., Díaz H.F. (Eds.), The Medieval Warm Period. Kluwer Academic Publishers. Dordrecht, The Netherlands, 342pp.

Huntley, B., Birks, H., 1983. An Atlas of Past and Present Pollen Maps for Europe: 0–13,000 Years Ago. Cambridge University Press, Cambridge, 667pp.

Hydrologic Engineering Center 1995. HEC-RAS, River Analysis System, Hydraulics Reference Manual, (CPD-69). Davis, California.

IPCC, 1996. Climate change 1995: impacts, adaptations, and mitigation of climate change: scientific-technical analyses. In: Watson,

R.T., Zinyowera, M.C., Moss, R.H. (Eds.), Contribution of Working Group II to the Second Assessment Report of the Intergovernmental Panel on Climate Change. Cambridge University Press, Cambridge, UK, New York, NY, USA, 880pp.

IPCC, 2001. Climate change 2001: impacts, adaptation and vulnerability. In: McCarthy, J.J., Canziani, O.F., Leary, N.A., Dokken D.J., White, K.S. (Eds.), Contribution of Working Group II to the Third Assessment Report of IPCC. Cambridge University Press, Cambridge, UK, New York, NY, USA, 1000pp.

Juliá, R., Guiralt, S., Burjachs, F., Roca, J.R., Wansard, G., 1998. Short climate events in the Mediterranean Iberian Peninsula during the Lateglacial and the Early Holocene transition. Terra Nostra 98 (6), 65–69.

Knox, J.C., 1983. Responses of river systems to Holocene climates. In: Wright, Jr. H.E. (Ed.), Late-Quaternary Environments of the United States, Vol. 2. University of Minnesota Press, Minneapolis, pp. 26–41.

Knox, J.C., 1985. Responses of floods to Holocene climatic change in the upper Mississippi Valley. Quaternary Research 23, 287–300.

Knox, J.C., 1993. Large increases in flood magnitude in response to modest changes in climate. Nature 361, 430–432.

Knox, J.C., 1999. Long-term episodic changes in magnitudes and frequencies of floods in the upper Mississippi River Valley. In: Brown, G.A., Quine, T.A. (Eds.), Fluvial Processes and Environmental Change. Wiley, New York, pp. 255–282.

Knox, J.C., 2000. Sensitivity of modern and Holocene floods to climate change. Quaternary Science Reviews 19, 439–457.

Kochel, R.C., Baker, V.R., Patton, P.C., 1982. Paleohydrology of Southwestern Texas. Water Resources Research 18, 1165–1183.

Lamb, H.F., Eicher, U., Switsur, V.R., 1989. An 18,000-year record of vegetational, lake level and climate change from the Middle Atlas, Morocco. Journal of Biogeography 16, 65–74.

Lamb, H.H., 1971. Climates and circulation regimes developed over the northern hemisphere during and since the Last Ice Age. Palaeogeography, Palaeoclimatology, Paleoecology 10, 125–162.

Martín-Arroyo, T., Ruiz-Zapata, M.B., 1996. Pollinic diagram of El Puente del Arzobispo slackwater flood deposits. In: Benito, G., Pérez-González, A., Machado, M.J., de Alba, S. (Eds.), Palaeohydrology and Modelling of Environmental Change. Second International Meeting on Global Continental Palaeohydrology. INQUA, Toledo, pp. 17–18.

Martín-Arroyo, T., Ruiz-Zapata, M.B., Pérez-González, A., Valdeolmillos, A., Dorado Valiño, M., Benito, G., Gil García, M.J., 1999. Paleoclima y paleoambiente durante el Pleistoceno Superior y el Tardiglaciar en la región central peninsular. In: Palli Buxó, L., Roqué Pau, C. (Eds.), Avances en el estudio del Cuaternario Español, Girona, pp. 317–324.

O'Connor, J.E., Ely, L.L., Wohl, E.E., Stevens, L.E., Meli, T.S., Kale, V.S., Baker, V.R., 1994. 4000-year record of large floods on the Colorado River in the Grand Canyon. Journal of Geology 102, 1–9.

Onate, J.J., Pou, A., 1996. Temperature variations in Spain since 1901: a preliminary analysis. International Journal of Climatology 16, 805–815.

Patton, P.C., Baker, V.R., Kochel, R.C., 1979. Slack-water deposits: a geomorphic technique for the interpretation of fluvial paleohydrology. In: Rhodes, D.D., Williams, G.P. (Eds.), Adjustments of the Fluvial System. Kendall Hunt Publ. Co., Dubuque, IA, pp. 225–252.

Peñalba, M.C., Arnold, M., Guiot, J., Duplessy, J.C., de Beaulieu, J.L., 1997. Termination of the Last Glaciation in the Iberian Peninsula inferred from the pollen sequence of Quintanar de la Sierra. Quaternary Research 48, 205–214.

Pérez Obiol, R., Juliá, R., 1994. Climatic change on the Iberian Peninsula recorded in a 30,000-yr pollen record from Lake Banyoles. Quaternary Research 41, 91–98.

Pickup, G., Allan, G., Baker, V.R., 1988. History, palaeochannels and palaeofloods of the Finke river, Central Australia. In: Warner, R.F. (Ed.), Fluvial Geomorphology of Australia. Academic Press, Australia, pp. 177–200.

Pons, A., Reille, M., 1988. The Holocene-and Upper Pleistocene pollen record from Padul (Granada, Spain): a new study. Palaeogeography, Palaeoclimatology, Palaeoecology 66, 243–263.

Porter, S.C., 1986. Pattern and forcing of Northern Hemisphere glacier variations during the Last Millennium. Quaternary Research 28, 27–48.

Ritchie, J.C., 1984. Analyse pollinique de sédiments Holocénes supérieurs des hauts plateaux du Maghreb Oriental. Pollen et Spores 26, 489–496.

Ruiz-Zapata, B., 1999. El Cambio Climático en la Península Ibérica. In: Ruiz-Zapata, B., Dorado, M., Gil, M.J., Valdeolmillos, A. (Eds.), Efectos del Cambio Climático en la Región Mediterránea durante los últimos 3000 años. Universidad de Alcalá de Henares, Madrid, pp. 86–95.

Roca, J.R., Juliá, R., 1997. Late glacial and holocene climatic changes and desertification expansion based on biota content in the Salines sequence, Southeastern Spain. Geobios 30, 823–830.

Starkel, L., 1991. Fluvial environments as a source of information on climatic changes and human impact in Europe. In: Frenzel, B., Pons, A., Gläser, B. (Eds.), Evaluation of Climate Proxy Data in Relation to the European Holocene. G. Fischer Verlag, Stuttgart, pp. 241–254.

Stuiver, M., Reimer, P.J., 1993. Extended 14C database and revised CALIB radiocarbon. Radiocarbon 35, 215–230.

Valero-Garcés, B., Kelts, K.R., 1997. Desertificación y Cambio Global en la Península Ibérica durante el último ciclo glacial a partir de registros lacustres. In: Ibáñez, J.J., Valero-Garcés, B.L., Machado, C. (Eds.), El paisaje mediterráneo a través del espacio y del tiempo. Implicaciones en la desertificación. Geoforma Ediciones, Logroño, pp. 419–437.

Valero-Garcés, B., Zeroual, E., Kelts, K., 1998. Arid Phases in the western Mediterranean region during the Last Glacial Cycle reconstructed from lacustrine records. In: Benito, G., Baker, V.R., Gregory, K.J. (Eds.), Palaeohydrology and Environmental Change. Wiley, London, pp. 67–80.

Valero-Garcés, B.L., González-Sampériz, P., Delgado-Huertas, A., Navas, A., Machín, J., Kelts, K., 2000. Lateglacial and Late Holocene environmental and vegetational change in Salada Mediana, central Ebro Basin, Spain. Quaternary International 73/74, 29–46.

Van der Brink, L.M., Janssen, C.R., 1985. The effects of human activities during cultural phases on the development of montane vegetation in the Serra de Estrela, Portugal. Review of Paleobotany and Palynology 44, 193–215.

Van der Knaap, W.O., van Leeuwen, J.F.N., 1995. Holocene vegetation succession and degradation as responses to climatic change and human activity in the Serra de Estrela, Portugal. Review of Paleobotany and Palynology, 153–211.

Wansard, G., Juliá, R., Roca, J.R., Riera, S., Seret, G., 1998. The last 2000 years-environmental change of Lake Estanya (NE Spain) based on mineralogy, ostracod fauna and trace-element shell chemistry. Terra Nostra 98, 132–136.

Webb, R.H., O'Connor, J.E., Baker, V.R., 1988. Paleohydrologic reconstruction of flood frequency on the Escalante River. In: Baker, V.R., Kochel, R.C., Patton, P.C. (Eds.), Flood Geomorphology. Wiley, New York, pp. 403–418.

Yang, D., Yu, G., Xie, Y., Zhan, D., Zhijia, L., 2000. Sedimentary records of large Holocene floods from the middle reaches of the Yellow River, China. Geomorphology 33, 73–88.

Zeroual, E., 1995. Enregistrements climatiques dans les sediments du Lac Isli (Haut Atlas du Maroc). Variations des influences climatiques sahariennes et mediterranéennes (de 34000 ans BP a nos jours). Ph.D. Thesis, University of Neuchatel, Switzerland.